Response to comments

Manuscript Number: acp-2017-23
Title: In situ chemical measurement of individual cloud residue particles at a mountain site, South China. Qinhao Lin et al.
Received and published: 20 March 2017

Anonymous Referee #1

Lin et al describe measurements of the chemistry of cloud droplet residues at a mountain-top site in South China in January 2016. Few measurements of cloud droplet residual chemistry exist, so these are important measurements to help improve our knowledge of cloud formation and properties, which are important for predicting weather and climate. Detailed comments follow.

We would like to thank the reviewer for his/her useful comments and recommendations to improve the manuscript. We agree with the comments, and careful revision has been made according to the suggestions.

It would be helpful for the authors to provide additional information about the cloud events. Please provide, at minimum, ambient temperature during the cloud events to justify the presence of cloud droplets only and no influence from ice crystals would be useful to discuss (related to Line 123); this is shown in Fig 1 and would be useful to refer to earlier to justify the presence of cloud droplets only.

We agree with the comments, and additional information has been added in the revised manuscript as suggested: Ambient temperature on average was 6.9 ℃ (ranging from -7.2 to 11.4 ℃) during the cloud events in this study. Therefore, the clouds here consisted of liquid droplets only. Please refer to Lines 124-126 of the revised manuscript.

It is stated on Line 135 that previous studies found an average cloud droplet size of 10 um at this site, but the distribution is not discussed, nor is the time of year of the previous measurements. Since this work is published in Chinese, these information are not easily obtained by the reader. So, additional discussion would be helpful.

Measurement of drop size spectrum in this region performed during winter of 1999-2001 shows that size of cloud droplets ranged from 4 to 25 μm, with average size of 10 μm and a corresponding liquid water content of 0.11-0.15 g m^{-3} (Deng et al., 2007). Some studies in other locations also showed an average size at ~10 μm (Freud et al.,

2008; Shingler et al., 2012). Therefore, it is reasonable to select a cut size at 8 μm for cloud droplets in the present study. The discussion has been added in section 2 as suggested, Please refer to Lines 126-131 of the revised manuscript.

Is it correct that measurements of cloud droplet size were not completed during this study? It would be helpful to know what fraction of the cloud droplet population was sampled, given the cut size of 8 um. For interpretation of the comparison between the cloud droplet residues and ambient particles, it is important to understand what fraction of the cloud droplets were measured. Previous studies (e.g. Bator & Collett 1997, J. Geophys. Res.) have found that cloud chemistry varies with droplet size. Sampling only the larger cloud droplets may also bias the cloud droplet residue size to larger particles, which is one of the observations. Since the cloud droplet activation process is also size-dependent, it is not possible for the reader to evaluate measurement vs droplet activation size dependencies currently.

It is true that measurements of cloud droplet size were not completed during this study. We agree with the comment. Sampling only the larger cloud droplets may also bias the cloud droplet residue size to larger particles. Previous measurements found that dust, playa salts or sea salt particles are often enriched in larger cloud droplets (~20 μm) (Bator and Collett, 1997; Pratt et al., 2010b). Organic carbon tends to be enriched in small cloud/fog droplets, extending to 4 μm (Herckes et al., 2013). It has been clarified that cloud droplets above 8 μm were sampled by the GCVI. Thus, it partially leads to relatively larger fractions of the Dust and Na-rich cloud residues observed, while the fraction of the OC cloud residues might be underestimated. Please refer to Lines 320-325 of the revised manuscript.

Major Comments:

Lines 20-23, lines 220-221, Figure 4, & numerous other locations: Do these number fractions take into account the size bias in the instrument inlet transmission efficiency, which is clear in Figure S3? It is clear that there are particle size dependencies to the cloud residual chemical composition, particularly for the amine and aged EC particle types, that should be considered when reporting fractions. For example, even on lines 220-221, it is not clear if the authors are reporting 3.8% of the total cloud residues, or 3.8% of the particles measured from 0.7-1.9 um, or 3.8% across each of the size bins from 0.7-1.9 um.

We agree with the comments. The chemical composition of cloud residues is dependent on the particle size (Roth et al., 2016), and the number reported for each particle type

might suffer the bias from size-dependent transmission efficiency (Qin et al., 2006). The relative fraction of cloud residues in 100 nm size interval is presented to minimize the size-dependent transmission efficiency of single particle mass spectrometry (Roth et al., 2016). Similarly, we have provided information on the number fractions of amine and aged EC particle types in cloud residues with size. Nf of the aged EC residues significantly decreased from 54.1% in the size range of 0.2-1.0 μm to 19.2% in the size range of 1.1-1.9 μm. The Amine particles contributed to 3.8% by number of the total cloud residues. Moreover, higher Nf of the Amine residues was detected in size range from 0.7 to 1.9 μm relative to size range from 0.2 to 0.6 μm (16.7% versus 0.4%). Please refer to Lines 20-23, 223-230 and 260-263 of the revised manuscript.

Lines 64-68: Only two other cloud studies are mentioned, or referenced, here, which incorrectly suggests to the reader that the measurement of anthropogenic particles in clouds has only been measured twice. While not all papers need to necessarily be referenced here, it is important to provide a comprehensive view to the reader.

We have added references (Stier et al., 2005; Sorooshian et al., 2007b; Lohmann et al., 2007; Rosenfeld et al., 2008; Roth et al., 2016; Seinfeld. et al., 2016; Li et al., 2017) to discuss the anthropogenic influence on cloud. Anthropogenic particles can increase number concentration of small cloud droplets, in turn, affect reflectivity and life time of clouds (Stier et al., 2005; Lohmann et al., 2007; Rosenfeld et al., 2008). In-situ cloud chemical measurements show varied chemical composition of cloud droplets at various regions (Sorooshian et al., 2007a; Roth et al., 2016; Li et al., 2017). Although a large number of aerosol/cloud studies over the past 20 years, the uncertainty for evaluating radiative forcing due to aerosol-cloud interactions has not been reduced (Seinfeld. et al., 2016). Please refer to Lines 55-62 of the revised manuscript.

Lines 87-89: This list is not comprehensive and is missing many papers. The authors are strongly suggested to conduct a detailed literature search, as comparison of their results with these papers is important.

We agree with the comment, and we have added related references about combined technique of a CVI and AMS or single particle measurement. These studies were mainly conducted in North America including Wyoming (Pratt et al., 2010a), Ohio (Hayden et al., 2008), Oklahoma (Berg et al., 2009), Florida (Cziczo et al., 2004; Twohy et al., 2005), California (Coggon et al., 2014), Europe including Schmücke (Roth et al., 2016; Schneider et al., 2017), Jungfraujoch (Kamphus et al., 2010), Åreskutan

(Drewnick et al., 2007), Scandinavia (Targino et al., 2006), Arctic (Zelenyuk et al., 2010), Central America (Cziczo et al., 2013), West Africa (Matsuki et al., 2010) and Oceans (Twohy et al., 2009; Twohy et al., 2008; Shingler et al., 2012). Please refer to Lines 81-88 of the revised manuscript.

Line 205 & Figure 3: Provide possible ion marker formulae here. Provide a reference for the aged EC type based on comparison to other single-particle mass spectrometry studies (e.g., reference to Moffet and Prather 2009, PNAS). Given the strong K+ signal here, it is likely that both the "Aged EC" and "K-rich" are from biomass burning. Similarly, the OC particles are likely aged biomass burning particles as well, given the strong K+ signal.

Possible ion marker formulae (m/z 27 $C_2H_3^+$, 43 $C_2H_3O^+$) were provided as suggested. We also noted that the aged EC type is similarly observed by other single-particle mass spectrometry studies (e.g., Moffet and Prather 2009, PNAS). We agree with the comment that the "Aged EC", "OC" and "K-rich" might be from biomass burning， as also discussed later. We have discussed the possibility, please refer to Lines 219-222, 232-233 and 314-315 of the revised manuscript.

Lines 209-210: The prevalence of wildfires, shown in Figure 2, suggests that these particles are primarily from biomass burning (see Pratt et al. 2011, ACP for a single particle mass spectrum of fresh biomass burning particles). Pratt et al. (2010, J. Atmos. Sci.) and Hudson et al. (2004, J. Geophys. Res.) discuss the identification of aged biomass burning particles by single-particle mass spectrometry. It seems that the authors can say with greater certainty the source of these particles, and discussion of this would elevate the paper by providing another evaluation of the influence of biomass burning aerosols on cloud activation, which is important and interesting.

We greatly appreciate the comment. Pratt et al (2011) has been cited here to identify the K-rich particles as biomass burning origin. Related references (Hudson et al., 2004; Pratt et al., 2010) were also cited to discuss the identification of aged biomass burning particles and to evaluate the influence of biomass burning aerosols on cloud activation. Majority of the K-rich cloud residues observed here are expected to originate from long-range transportation. Aging process during long-range transportation can increase soluble species (e.g., sulfate, nitrate and oxalate) in the K-rich particles, in turn, improve CCN activity. Please refer to Lines 232-238 and 464-468 of the revised manuscript.

Lines 221-227: It is not clear if Roth et al. observed a decreased fraction of amines in

the clouds compared to the ambient, or if amines just do not influence the site. The presence and behavior of amines would be location and season dependent, so this discussion is not clear and seems to be comparing studies without considering commonalities.

We agree with the comment that the presence and behavior of amines would be location and season dependent. We have made it clear by comparing an Nf of amine-containing aerosol between cloud residues and background aerosol (9% versus 2% by number) in Roth et al. (2016). It indicates a preferential formation of amine in cloud. Aqueous reaction improving the participation of amine has been observed in Guangzhou (Zhang et al., 2012a) and Southern Ontario (Rehbein et al., 2011). Please refer to Lines 263-267 of the revised manuscript.

Lines 244-247: To further understand the source of the Na-rich particles, were they present for both coastal and non-coastal wind directions? Is there a difference in the average mass spectra for these wind directions considering the minor peaks? Are industrial sources located in both directions?

Na-rich particles were resulted from varied sources, including industrial emissions, sea salt or dry lake beds (Moffet et al. 2008). The Nf of the Na-rich cloud residues did not increase from continental (Northerly) air mass to maritime (southwesterly) air mass on 21 Jan (3.3% versus 2.4% by number). However, related sea salt ion peak area (m/z, 81/83$Na_2{}^{35}Cl/Na_2{}^{37}Cl$) were enhanced for Na-rich particles origination from maritime air mass relative to continental air mass (3.8 ± 2.4 times). Continental air masses crossed industrial areas where located in the Yangtze River Mid-Reaches city cluster (Figure 2). Industrial emissions was a possible contributor to Na-rich particles under the influence of continental air masses (Wang et al. 2016). This might suggests that the Na-rich particles were contributed by both the industrial emissions and sea salt. Therefore, under the influence of maritime air mass, the signals for sea salt contribution became stronger. Please refer to Lines 299-310 of the revised manuscript.

Lines 263-267: While ammonium nitrate does not contribute to the dust nitrate observed here, it is not appropriate to generalize this statement to suggest that previous studies in other very different locations did not measure ammonium nitrate.

We agree with the comment. We have revised this sentence to "in this region, ammonium nitrate was not a predominant form of nitrate in the Dust cloud residues", to make it clear. Please refer to Lines 339-340 of the revised manuscript.

Lines 319-329: Was there a mass spectral difference in the K-rich particle type between the N and SW wind directions that would aid in source identification for the two air masses?

A similarity in averaged mass spectrum of the K-rich residues was found for the southwesterly and northerly air masses (Figure S6). Please refer to Lines 419-420 of the revised manuscript.

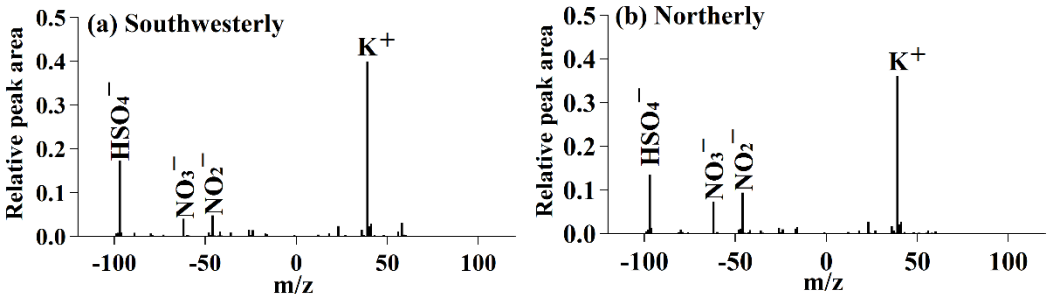

Figure S6: Average mass spectra of K-rich residues for southwesterly (a) and northerly (b) air masses.

Section 3.6: This authors should consider incorporating this discussion into the other sections of the manuscript so that comparisons are made when results are discussed. In addition, the authors should consider differences in atmospheric composition at the various sites. when discussing specific comparisons (i.e. are the contributing sources and magnitudes the same, or may this be a reason for differences? Or, are the seasons the same?). Currently only a general statement on lines 431-433 states that differences are specific to geographic location. As noted above, the literature cited is also not comprehensive, and this section would benefit from additional literature searching.

We agree with the comment. We have incorporated this discussion into the other sections of the manuscript. We have also discussed same or different reason for sources and magnitudes of cloud residues at various sites. We have also cited related literatures (Drewnick et al., 2007; Twohy et al., 2008; Twohy et al., 2009; Matsuki et al., 2010; Kamphus et al., 2010; Pratt et al., 2010b; Zelenyuk et al., 2010; Roth et al., 2016; Bi et al., 2016). Please refer to Lines 241-253, 273-275, 464-471, 489-494 and 505-509 of the revised manuscript.

Figure 4: It would be useful to add comparisons to the ambient and interstitial particles here. In addition, since the cloud residue types changed significantly based on air mass

origin (N vs SW), as stated in Section 3.4, it would be useful to separate out these wind directions and show the fractions of cloud residue, interstitial, and ambient, separated for the two wind directions.

We agree with the the comment. The fractions of the ambient and non-activated particles were provided in Figure 7. The fractions of cloud residue in comparison to ambient particles was performed based on northerly air mass. Please refer to section 3.4 of the revised manuscript.

During the sampling period, the cloud events occurred once the southwesterly air masses were dominant. Therefore, a comparison between cloud residues and ambient particles cannot be addressed under the influence of southwesterly air masses. Please refer to Lines 445-448 of the revised manuscript.

A comparison of cloud residues and non-activated particles has been performed. However, from 22 to 23 Jan during cloud III events, the air mass encountered initial mixing of cloud-free air originated from north and cloudy air originated from southwest. Therefore, a comparison of cloud residues and non-activated particles was not performed for a special wind direction during cloud III events. Please refer to section 3.5 of the revised manuscript.

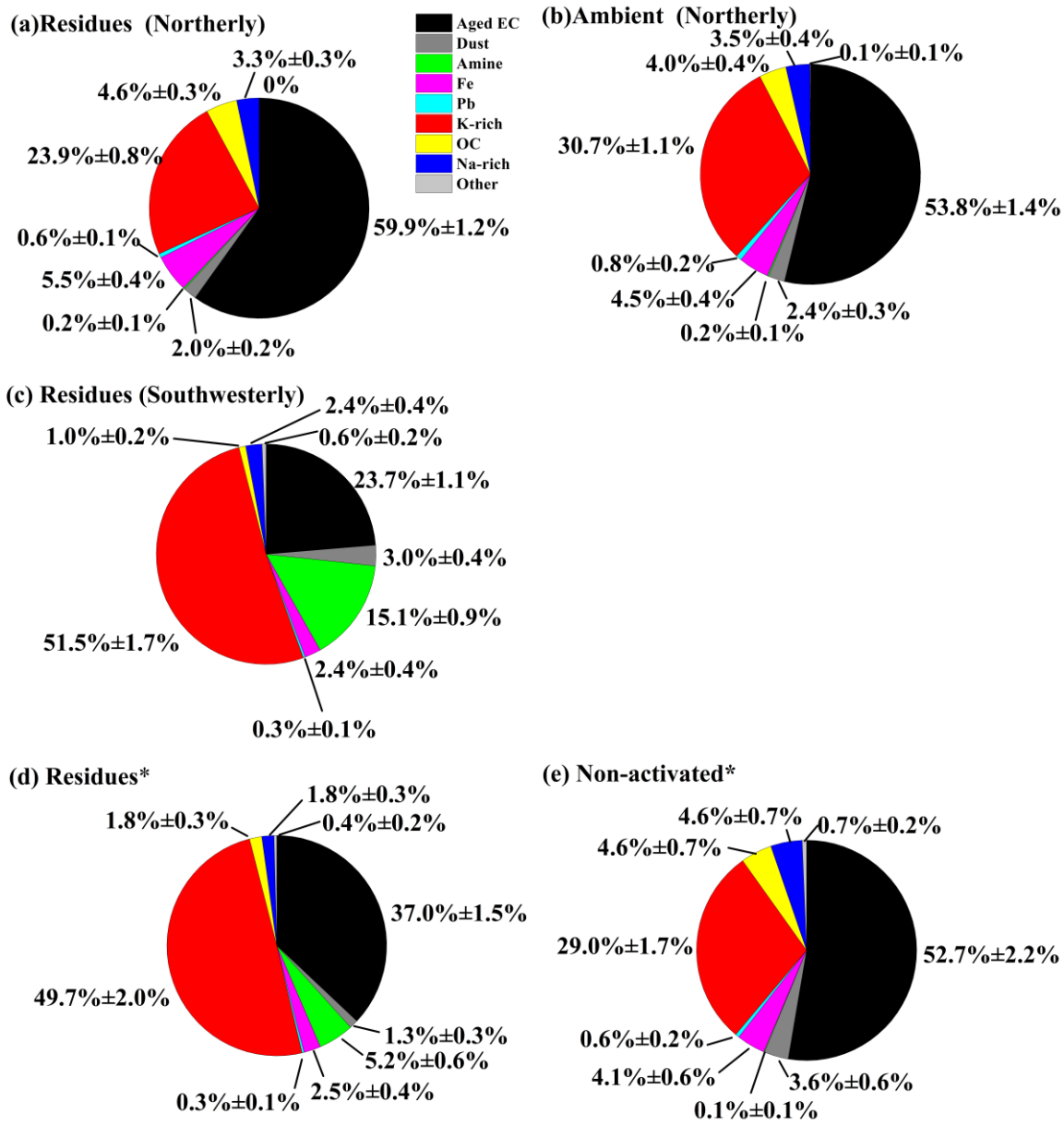

Figure 7: Number fraction of the cloud residues, ambient and non-activated particles. (a) cloud residues during northerly air mass; (b) ambient particle during northerly air mass; (c) cloud residues during southwesterly air mass; (d) cloud residues and (e) non-activated particles were alternately sampled with interval of one hour during the cloud III event; Uncertainties were calculated assuming Poisson statistics for analyzed particles.

Technical Comments:

Lines 24-26, 45, & other locations (search document): Please clarify what is meant by "intensity" in these statements.

Intensity refers to average ion peak area. We have clarified them. Please refer to Lines 24, 43-44 and 486 of the revised manuscript.

Lines 29-30: The phrase "To estimate how atmospheric aerosol particles respond to chemical properties of cloud droplets" is not clear since aerosols determine cloud droplet chemistry, outside of aqueous processing from dissolved trace gases.

The phrase has been changed to " To estimate how atmospheric aerosol particles interact with chemical composition of cloud". Please refer to Line 27 of the revised manuscript.

Lines 41-42: For readers not familiar with the region, it would be helpful to know the suggested source of the amine particles, which the authors are presumably referring to with respect to the wind direction change.

Sources of the amine particles (e.g., ocean and livestock areas) were provided under the influence of southwesterly air masses. Please refer to Lines 40 of the revised manuscript.

Line 44: What does "highly associated" mean in this context? This phrase occurs in other locations in the manuscript as well.

We have modified them. Higher Nfs of nitrate (88-89%) were found in the Dust and Na-rich cloud residues relative to sulfate (41-42%) and ammonium (15-23%). Please refer to Lines 41-43 and 530-532 of the revised manuscript.

Lines 76-80: This sentence incorrectly cites Pratt et al 2010a for cloud droplet residues. The authors should also consider Drewnick et al 2007, J. Atmos. Chem., who did observe lower sulfate mass fractions for droplet residues compared to ambient aerosol. Pratt et al 2010 (J. Geophs. Res.) shows increased mixing with sulfate/nitrate for liquid clouds, compared to ice clouds, as another example.

We have deleted the citation of Pratt et al 2010a and added a citation of Drewnick et al 2007 here. Please refer to Lines 74-75 of the revised manuscript.

A comparison of liquid clouds and ice clouds is beyond the scope of this work, Pratt et

al 2010 (J. Geophs. Res.) was not cited here.

Line 161: It should be clarified that "cloud droplet residue concentrations", not "cloud droplet concentrations" were measured by the SMPS. This is an important distinction.

We have corrected "cloud droplet concentration" to "cloud residual concentration" throughout the manuscript. Please refer to Lines 165-168 of the revised manuscript.

Lines 163-165: Wouldn't hazy days with low visibility be characterized by high, rather than low, PM2.5 concentrations? This is confusing.

Low level of $PM_{2.5}$ (~ 12.7 μg m^{-3}) excludes the influence of hazy days. Please refer to Lines 169-170 of the revised manuscript.

Line 165: Change "rainy" to "rain".

We have changed "rainy" to "rain" accordingly. Please refer to Line 171 of the revised manuscript.

Line 216: It is important to consider the relative enhancement in amine peaks when using a 266 nm laser and that the amines themselves may not comprise the majority of the particle mass. See Pratt et al. 2009, Environ. Sci. Technol.

We have emphasized the effect of 266 nm ionization laser on amine peaks (Pratt et al., 2009). Please refer to Lines 257-259 of the revised manuscript.

Lines 230-232: It should be clarified when discussing previous vs the current study, and if previous studies are being discussed, the season should be noted if there are seasonal variations.

We agree with the comments. We have clarified the specific season in the discussion. At Mt. Tai in northern China, a high concentration of Ca^{2+} in cloud/fog water was mainly attributed to a sandstorm event during spring season (Wang et al., 2011). At Mt. Heng in southern China, abundant crust-related elements (e.g., Al) observed in cloud water is due to Asian dust storms occurring on March−May (Li et al., 2017). Based on backward trajectory, the site in this study was less affected by sandstorm source in northwestern China during cloud events. Local dust emission by anthropogenic-disturbing soils or removing vegetation cover can be excluded as a result of forest

protection. Therefore, a low fraction (2.9% by number) of dust cloud residue is acceptable in the present study. Please refer to Lines 278-287 of the revised manuscript.

Lines 231-237: Some grammar fixes are needed here.

The language has been edited by a native speaker.

Line 279: Please be more specific with the statement "plays a key role in cloud processes". you mean that these particles were preferentially activated? Is there evidence of this?

We have reworded this sentence: "This result also implies that ammonium-containing particles are preferentially activated or enhanced by uptake of gaseous NH_3 to neutralize acidic cloud droplets for the OC and EC types. Please refer to Lines 354-356 of the revised manuscript.

Lines 358-396: The phrasing in these paragraphs should be improved for greater clarity and correct grammar.

These paragraphs have been reworded. Please refer to Lines 463-509 of the revised manuscript.

Line 390: This is an important finding, yet the phrasing "sulfate was observed to diminish" not clear, particularly when considering the following sentence. Please clarify.

We have rephrased and changed to "sulfate intensity was observed to diminish". Please refer to Lines 502-503 of the revised manuscript.

Lines 395-396: What discrepancy? This is not clear.

The discrepancy refers to "the mass or number fraction of sulfate-containing particles in the cloud residues changed between ambient and interstitial (non-activated) particles (Drewnick et al., 2007; Twohy and Anderson, 2008; Schneider et al., 2017)". We have changed "this discrepancy" to "these changes" to make it clear. Please refer to Lines 505-509 of the revised manuscript.

Line 397: Quantitatively, what is "no remarkable change"? The phrase "remarkable

change" is used elsewhere in the manuscript as well, but it isn't defined.

"no remarkable change": We added the data on number factions when the residual particles were compared with ambient or non-activated particles. "remarkable change" has been modified to "remarkable decrease/increase" and added the data on number factions when the residual particles were compared with ambient or non-activated particles. Please refer to Lines 511-513 and 518-519 of the revised manuscript.

Table 2: Not sure what the authors mean by "way" here.

"way" : Cloud residues and non-activated particles were alternately sampled with interval of one hour during the cloud III event. Table 2 has been replaced by pie charts in Figure 7. Please refer to Lines 452-453 of the revised manuscript and the caption of Figure 7.

Figure 2: The lines and numbers on this map are difficult to read. It would be useful to make the text bold perhaps and increase the width of the lines.

We have changed accordingly. Please refer to the modified Figure 2a.

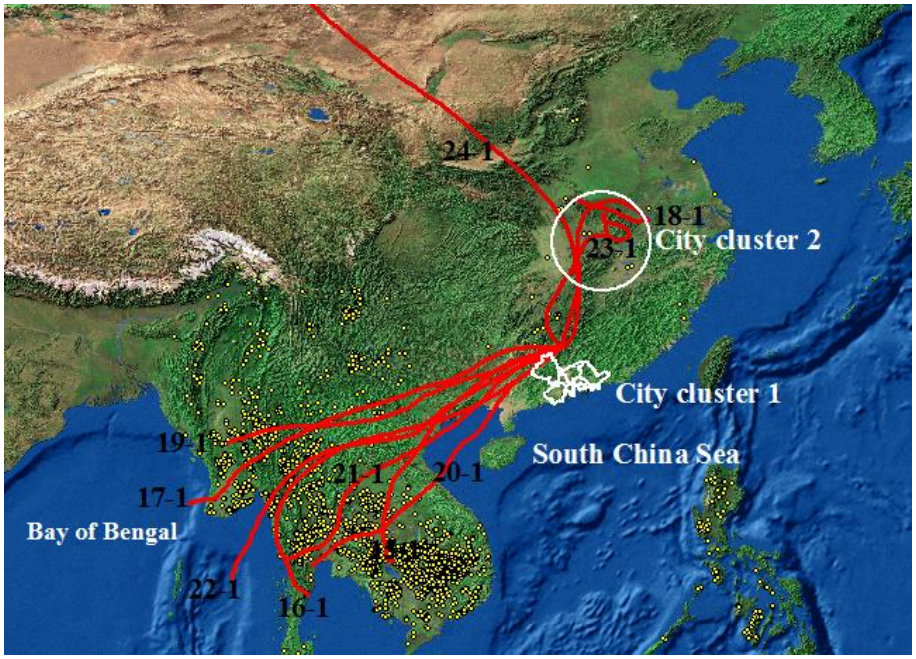

Figure 3: This plot is difficult to read. The authors should consider showing only the most abundant (and discussed) particle types in the main text figure and moving the others (including "Other", which is somewhat meaningless as an average mass spectrum if it is made up of a diverse population of particles) to the supplemental

information.

We have improved Figure 3 resolution. Please refer to the modified Figure 3. Average mass spectrum of Pb, OC and Other types have been moved to the supplemental information (Figure S4)

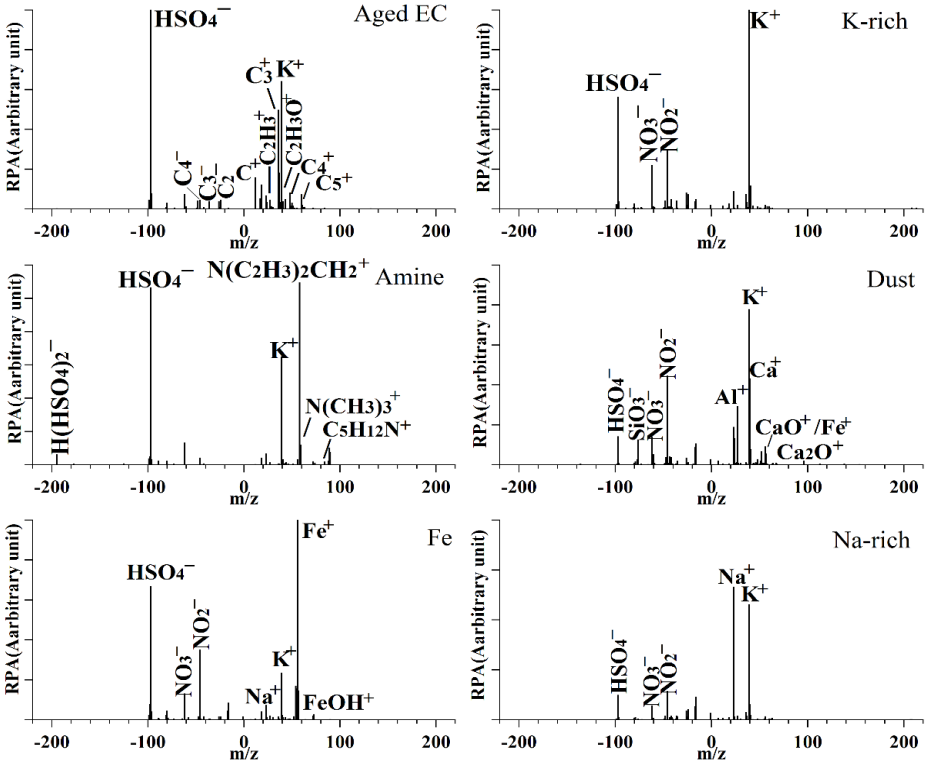

Figure 3: Averaged positive and negative mass spectra for the main 6 particle types (Aged EC, K-rich, Amine, Dust, Fe, Na-rich) of the sampled particles during the whole sampling period. RPA in the vertical axis refers to relative peak area. m/z in the horizontal axis represents mass-to-charge ratio.

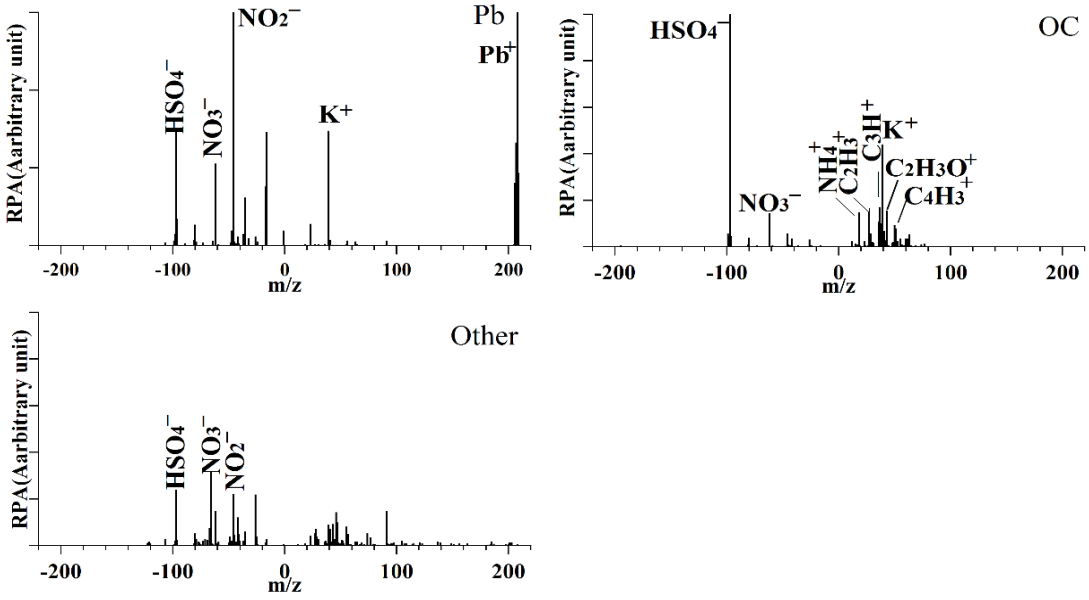

Figure S4: Averaged positive and negative mass spectra for Pb, OC and Other types of the sampled particles during the whole sampling period. RPA in the vertical axis refers to relative peak area. m/z in the horizontal axis represents mass-to-charge ratio.

Figures 7 and 8: Please indicate whether positive peak areas indicate preferentially in the cloud residues and negative indicate preferentially in the ambient/interstitial particles. This is currently not clear in the figure captions.

We have clarified them in the captions of Figures 8 and 9 of the revised manuscript.
Figure 8: Mass spectral subtraction plot of the average mass spectrum corresponding to cloud residues minus ambient particles. Positive peak area corresponds to higher abundance in cloud residues, whereas negative peak area show higher intensity in ambient particles.
Figure 9: Mass spectral subtraction plot of the average mass spectrum corresponding to cloud residues minus non-activated particles. Positive peak area correspond to higher abundance in cloud residues, whereas peak area show higher intensity in non-activated particles.

Figure S4: It is not clear in the maps where RH < and > 90% are located.

We have added contour lines of two relative humidity (50%, 70%) in the Figure S5. Please refer to the modified Figure S5.

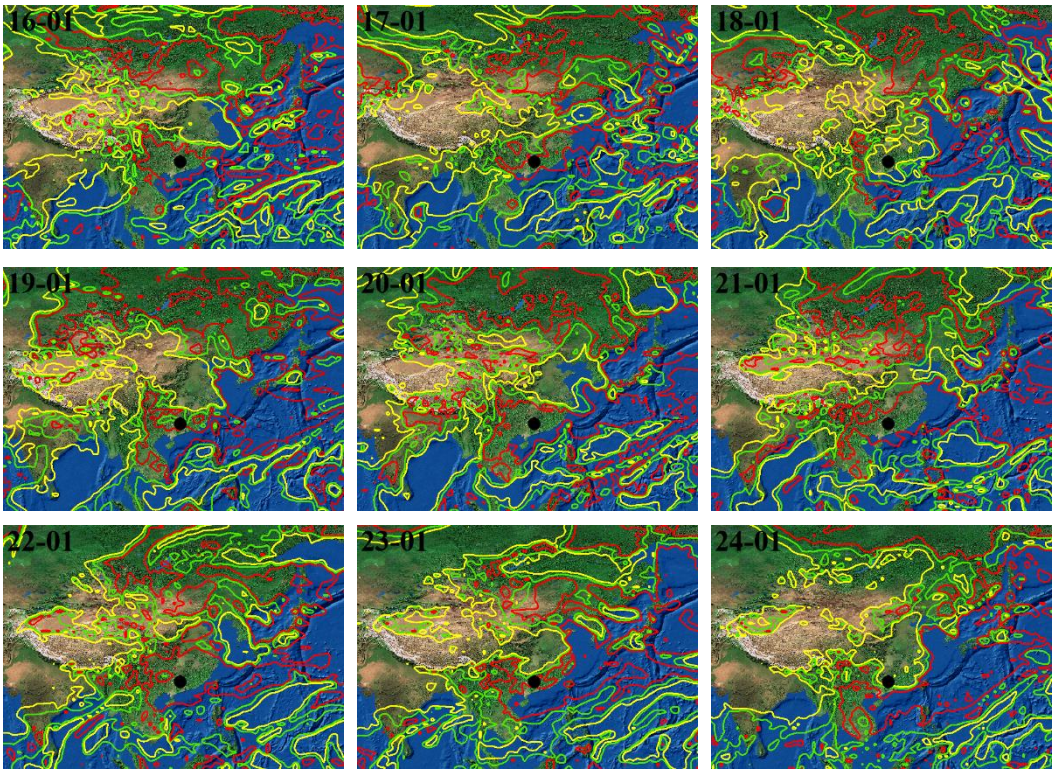

Figure S5: At 850 hPa (about 1,500 m a.s.l), Contour lines (red lines) of relative humidity 90%; Contour lines (green lines) of relative humidity 70%; Contour lines (yellow lines) of relative humidity 50%. Black mark represents the observed site. Data is available at ftp://arlftp.arlhq.noaa.gov/pub/archives/gdas1/.

References:

Bator, A. and Collett, J.L.: Cloud chemistry varies with drop size, J. Geophys. Res. Atmos., 102, 28071-28078. 1997.

Berg, L.K., Berkowitz, C.M., Hubbe, J.M., Ogren, J.A., Hostetler, C.A., Ferrare, R.A., Hair, J.W., Dubey, M.K., Mazzoleni, C. and Andrews, E.: Overview of the cumulus humilis aerosol processing study, B. Am. Meteorol. Soc. 90, 1653-1667, 2009.

Bi, X., Lin, Q., Peng, L., Zhang, G., Wang, X., Brechtel, F. J., Chen, D., Li, M., Peng, P. a., Sheng, G. and Zhou, Z.: In situ detection of the chemistry of individual fog droplet residues in the Pearl River Delta region, China, J. Geophys. Res. Atmos., 121, 9105-9116, 2016.

Coggon, M.M., Sorooshian, A., Wang, Z., Craven, J.S., Metcalf, A.R., Lin, J.J., Nenes, A., Jonsson, H.H., Flagan, R.C., Seinfeld, J.H.: Observations of continental biogenic impacts on marine aerosol and clouds off the coast of California, J. Geophys. Res. Atmos., 119, 6724-6748, 2014.

Cziczo, D.J., Froyd, K.D., Hoose, C., Jensen, E.J., Diao, M., Zondlo, M.A., Smith, J.B., Twohy, C.H., Murphy, D.M.: Clarifying the dominant sources and mechanisms of cirrus cloud formation,

Science, 340, 1320-1324, 2013.

Cziczo, D.J., Murphy, D.M., Hudson, P.K., Thomson, D.S.: Single particle measurements of the chemical composition of cirrus ice residue during CRYSTAL-FACE, J. Geophys. Res. Atmos., 109, D04201, doi:10.1029/2003JD004032, 2004.

Deng, X., Wu, D., Shi, Y., Tang, H., Fan, S., Huang, H., Mao, W. and Ye, Y.: Comprehensive analysis of the macro-and micro-physical characteristics of dense fog in the area south of the Nanling Mountains (in Chinese), J.Trop. Meteorol., 23, 424-434. 2007,

Drewnick, F., Schneider, J., Hings, S. S., Hock, N., Noone, K., Targino, A., Weimer, S., and Borrmann, S.: Measurement of ambient, interstitial, and residual aerosol particles on a mountaintop site in central Sweden using an aerosol mass spectrometer and a CVI, J. Atmos. Chem., 56, 1-20, 2007.

Freud, E., Rosenfeld, D., Andreae, M.O., Costa, A.A. and Artaxo, P.: Robust relations between CCN and the vertical evolution of cloud drop size distribution in deep convective clouds, Atmos. Chem. Phys., 8, 1661-1675, 2008.

Herckes, P., Valsaraj, K.T. and Collett, J.L.: A review of observations of organic matter in fogs and clouds: Origin, processing and fate, Atmos. Res., 132, 434-449. 2013.

Hudson, P.K., Murphy, D.M., Cziczo, D.J., Thomson, D.S., de Gouw, J.A., Warneke, C., Holloway, J., Jost, H.J., Hübler, G.: Biomass-burning particle measurements: Characteristic composition and chemical processing, J. Geophys. Res. Atmos., 109, D23S27, doi:10.1029/2003JD004398, 2004.

Kamphus, M., Ettner-Mahl, M., Klimach, T., Drewnick, F., Keller, L., Cziczo, D. J., Mertes, S., Borrmann, S., and Curtius, J.: Chemical composition of ambient aerosol, ice residues and cloud droplet residues in mixed-phase clouds: single particle analysis during the Cloud and Aerosol Characterization Experiment (CLACE 6), Atmos. Chem. Phys., 10, 8077-8095, 2010.

Li, T., Wang, Y., Zhou, J., Wang, T., Ding, A., Nie, W., Xue, L., Wang, X. and Wang, W.: Evolution of trace elements in the planetary boundary layer in southern China: effects of dust storms and aerosol-cloud interaction, J. Geophys. Res. Atmos., 122, 3492-3506, 2017.

Lohmann, U., Stier, P., Hoose, C., Ferrachat, S., Kloster, S., Roeckner, E., Zhang, J.: Cloud microphysics and aerosol indirect effects in the global climate model ECHAM5-HAM, Atmos. Chem. Phys., 7, 3425-3446, 2007.

Matsuki, A., Schwarzenboeck, A., Venzac, H., Laj, P., Crumeyrolle, S., Gomes, L.: Cloud processing of mineral dust: direct comparison of cloud residual and clear sky particles during AMMA aircraft campaign in summer 2006. Atmos. Chem. Phys., 10, 1057-1069, 2010.

Moffet, R.C., Foy, B. d., Molina, L. a., Molina, M., and Prather, K.: Measurement of ambient aerosols in northern Mexico City by single particle mass spectrometry, Atmos. Chem. Phys., 8, 4499-4516, 2008.

Moffet, R.C., Prather, K.A.: In-situ measurements of the mixing state and optical properties of soot with implications for radiative forcing estimates, Proc. Natl. Acad. Sci. USA, 106, 11872-

11877, 2009.

Pratt, K. A., Hatch, L. E., and Prather, K. A.: Seasonal volatility dependence of ambient particle phase amines, Environ. Sci. Technol., 43, 5276-5281, 2009.

Pratt, K. A., Heymsfield, A. J., Twohy, C. H., Murphy, S. M., DeMott, P. J., Hudson, J. G., Subramanian, R., Wang, Z., Seinfeld, J. H., and Prather, K. A.: In Situ Chemical Characterization of Aged Biomass-Burning Aerosols Impacting Cold Wave Clouds, J. Atmos. Sci., 67, 2451-2468, 2010a.

Pratt, K.A., Murphy, S., Subramanian, R., DeMott, P., Kok, G., Campos, T., Rogers, D., Prenni, A., Heymsfield, A., Seinfeld, J.: Flight-based chemical characterization of biomass burning aerosols within two prescribed burn smoke plumes, Atmos. Chem. Phys., 11, 12549-12565, 2011.

Pratt, K.A., Twohy, C.H., Murphy, S.M., Moffet, R.C., Heymsfield, A.J., Gaston, C.J., DeMott, P.J., Field, P.R., Henn, T.R., Rogers, D.C., Gilles, M.K., Seinfeld, J.H., Prather, K.A.: Observation of playa salts as nuclei in orographic wave clouds. J. Geophys. Res.Atmos., 115, doi:10.1029/2009JD013606, 2010b.

Qin, X., Bhave, P.V. and Prather, K. A.: Comparison of two methods for obtaining quantitative mass concentrations from aerosol time-of-flight mass spectrometry measurements, Anal. Chem., 78(17), 6169-6178, doi: 10.1021/ac060395q, 2006.

Rehbein, P. J., Jeong, C. H., McGuire, M. L., Yao, X., Corbin, J. C., and Evans, G. J.: Cloud and fog processing enhanced gas-to-particle partitioning of trimethylamine, Environ. Sci. Technol., 45, 4346-4352, doi:10.1021/es1042113, 2011.

Rosenfeld, D., Lohmann, U., Raga, G.B., O'Dowd, C.D., Kulmala, M., Fuzzi, S., Reissell, A., Andreae, M.O.: Flood or drought: how do aerosols affect precipitation? Science, 321, 1309-1313, 2008.

Roth, A., Schneider, J., Klimach, T., Mertes, S., van Pinxteren, D., Herrmann, H., and Borrmann, S.: Aerosol properties, source identification, and cloud processing in orographic clouds measured by single particle mass spectrometry on a central European mountain site during HCCT-2010, Atmos. Chem. Phys., 16, 505-524, 2016.

Schneider, J., Mertes, S., van Pinxteren, D., Herrmann, H., and Borrmann, S.: Uptake of nitric acid, ammonia, and organics in orographic clouds: Mass spectrometric analyses of droplet residual and interstitial aerosol particles, Atmos. Chem. Phys., 17, 1571-1593, 2017.

Seinfeld, J.H., Bretherton, C., Carslaw, K.S., Coe, H., DeMott, P.J., Dunlea, E.J., Feingold, G., Ghan, S., Guenther, A.B., Kahn, R.: Improving our fundamental understanding of the role of aerosol-cloud interactions in the climate system. Proc. Natl. Acad. Sci. USA, 113, 5781-5790, 2016.

Sorooshian, A., Ng, N. L., Chan, A. W. H., Feingold, G., Flagan, R. C., and Seinfeld, J. H.: Particulate organic acids and overall water-soluble aerosol composition measurements from the 2006 Gulf of Mexico Atmospheric Composition and Climate Study (GoMACCS), J. Geophys. Res. Atmos., 112(D13), doi:10.1029/ 2007JD008537, 2007a.

Shingler, T., Dey, S., Sorooshian, A., Brechtel, F. J., Wang, Z., Metcalf, A., Coggon, M.,

Mülmenstädt, J., Russell, L. M., Jonsson, H. H. and Seinfeld, J. H.: Characterisation and airborne deployment of a new counterflow virtual impactor inlet, Atmos. Meas. Tech., 5, 1259-1269, doi:10.5194/amt-5-1259-2012, 2012.

Stier, P., Feichter, J., Kinne, S., Kloster, S., Vignati, E., Wilson, J., Ganzeveld, L., Tegen, I., Werner, M., Balkanski, Y.: The aerosol-climate model ECHAM5-HAM. Atmos. Chem. Phys., 5, 1125-1156. 2005.

Tang, M., Cziczo, D. J., and Grassian, V. H.: Interactions of Water with Mineral Dust Aerosol: Water Adsorption, Hygroscopicity, Cloud Condensation, and Ice Nucleation, Chem. Rev., doi:10.1021/acs.chemrev.5b00529, 2016.

Targino, A.C., Krejci, R., Noone, K.J., Glantz, P.: Single particle analysis of ice crystal residuals observed in orographic wave clouds over Scandinavia during INTACC experiment, Atmos. Chem. Phys., 6, 1977-1990, 2006.

Twohy C.H. and Anderson J. R.: Droplet nuclei in non-precipitating clouds: composition and size matter. Environ. Res. Lett., 3, 045002, doi:10.1088/1748-9326/3/4/045002, 2008.

Twohy, C.H., Kreidenweis, S.M., Eidhammer, T., Browell, E.V., Heymsfield, A.J., Bansemer, A.R., Anderson, B.E., Chen, G., Ismail, S., DeMott, P.J., Van Den Heever, S.C.: Saharan dust particles nucleate droplets in eastern Atlantic clouds, Geophys. Res. Lett. 36, doi: 10.1029/2008GL035846, 2009.

Twohy, C.H., Poellot, M.: Chemical characteristics of ice residual nuclei in anvil cirrus clouds: evidence for homogeneous and heterogeneous ice formation, Atmos. Chem. Phys., 5, 2289-2297, 2005.

Wang, H., An, J., Shen, L., Zhu, B., Xia, L., Duan, Q. and Zou, J.: Mixing state of ambient aerosols in Nanjing city by single particle mass spectrometry, Atmos. Environ., 132, 123-132, 2016.

Wang, Y., Guo, J., Wang, T., Ding, A., Gao, J., Zhou, Y., Collett, J. L., and Wang, W.: Influence of regional pollution and sandstorms on the chemical composition of cloud/fog at the summit of Mt. Taishan in northern China, Atmos. Res., 99, 434-442, 2011.

Zelenyuk, A., Imre, D., Earle, M., Easter, R., Korolev, A., Leaitch, R., Liu, P., Macdonald, A. M., Ovchinnikov, M., and Strapp, W.: In Situ Characterization of Cloud Condensation Nuclei, Interstitial, and Background Particles Using the Single Particle Mass Spectrometer, SPLAT II†, Anal. Chem., 82, 7943-7951, 2010.

Zhang, G., Bi, X., Chan, L. Y., Li, L., Wang, X., Feng, J., Sheng, G., Fu, J., Li, M., and Zhou, Z.: Enhanced trimethylamine-containing particles during fog events detected by single particle aerosol mass spectrometry in urban Guangzhou, China, Atmos. Environ., 55, 121-126, doi:10.1016/j.atmosenv.2012.03.038, 2012a.

Response to comments

Manuscript Number: acp-2017-23
Title: In situ chemical measurement of individual cloud residue particles at a mountain site, South China. Qinhao Lin et al.
Received and published: 20 March 2017

Referee #2: J. Schneider

In their manuscript "In situ chemical measurement of individual cloud residue particles at a mountain site, South China", Qinhao Lin and co-workers report on the analysis of single particles from cloud residues using a single particle aerosol mass spectrometer. They observed a high fraction of EC-containing particle in the residuals and detected amines with a high variability. Nitrate was found to be increased in residuals compared to ambient particles, while sulfate showed a dependency on the chemical composition of the residues. The topic of the paper is well suited for ACP, and the data itself are interesting, because single particle measurements of cloud residuals are still sparse. However, the manuscript suffers from many unclear statements and some severe uncertainties regarding the analysis of interstitial particles. I have many points where more information is needed or where I disagree. None of these points alone would be a "major" comment, but the multitude of my remarks and questions suggest to require a major revision and to reconsider the manuscript after my comments listed below have been addressed.

We would like to thank Prof. J. Schneider for his useful comments and recommendations to improve the manuscript. We agree with the comments, and careful revision has been made accordingly, please refer to the following responses for details.

Comments and remarks:
Title: I suggest to change the title to "In situ chemical composition measurement of individual cloud residue particles at a mountain site, South China"

We have changed accordingly. Please refer to Lines 1-2 of the revised manuscript.

Page 4, lines 64 – 68:
More references are needed here to discuss the anthropogenic influence on cloud particles, not just two papers on single particle analysis.

As also suggested by Reviewer 1, We have added references (Stier et al., 2005; Sorooshian et al., 2007b; Lohmann et al., 2007; Rosenfeld et al., 2008; Roth et al., 2016; Seinfeld. et al., 2016; Li et al., 2017) to discuss the anthropogenic influence on cloud particles. Anthropogenic particles can increase number concentration of small cloud droplets, in turn, affect reflectivity and life time of clouds (Rosenfeld et al., 2008; Stier et al., 2005; Lohmann et al., 2007). In-situ cloud chemical measurements show varied chemical composition of cloud droplets at various regions (Sorooshian et al., 2007a; Roth et al., 2016; Li et al., 2017). Although a large number of aerosol/cloud studies over the past 20 years, the uncertainty for evaluating radiative forcing due to aerosol-cloud interactions has not been reduced (Seinfeld. et al., 2016). Please refer to Lines 55-62 of the revised manuscript.

Page 5, line 79: Replace "Nf of sulfate" by "NF of sulfate-containing particles"

We have changed it accordingly. Please refer to Line 74 of the revised manuscript.

Page 5, line 80: Replace "other study" by "other studies"

We have changed it accordingly. Please refer to Line 76 of the revised manuscript.

Page 7, line 122: Was the humidity measured in the evaporation chamber? How do you make sure that all water evaporates?

Relative humidity (RH) was around 30% in the evaporation chamber, thus it can be assumed that the majority of water was evaporated. Please refer to Lines 131-134 of the revised manuscript.

Page 8, lines 147-149: Did you do the size calibration on the mountain top station? What was the ambient pressure during the measurements and during the calibration? Did you check the inlet flow or the pressure inside the aerodynamic lens?

We did the size calibration on the mountain top station. Polystyrene latex spheres (Nanosphere Size Standards, Duke Scientific Corp., Palo Alto) of 0.2-2.0 μm in diameter were used to calibrate the sizes of the detected particles on the mountain top station. The ambient pressure was 830 hPa (826-842 hPa) during the measurements and during the

calibration. The pressure inside the aerodynamic lens maintains about 3 hPa during the measurements and during the calibration. Please refer to Lines 152-155 of the revised manuscript.

Page 8, line 161: The SMPS does not measure the cloud droplet concentration but the cloud residue concentration. Cloud droplets would have to be measured outside in the cloud (by FSSP or similar instrumentation).

We have corrected the mistake. "cloud droplet concentration" was replaced with "cloud residual concentration". Please refer to Lines 165-168 of the revised manuscript.

Page 9, line 171: As I will outline in more detail below, I doubt the existence of interstitial particles in this size range.

The period of collecting interstitial particles on 22-23 Jan encountered initial mixing of northerly cloud-free air (dry and cold airstreams) and southwesterly cloudy air (moist airflows). The dry northern air mass might lower supersaturation, only larger particles could be activated. This might result in non-activated particles observed to be above 200 nm here (Mertes et al., 2005; Kleinman et al., 2012; Hammer et al., 2014). To make it more accurate, we prefer to name "non-activated particles", rather than "interstitial particles". We have clarified them. Please refer to Lines 452-461 of the revised manuscript.

Page 9 lines 184-185 and Figure 2: More info on the trajectories is needed: How did the vertical evolution look like? How well is the mountain represented in the model? Is 1800 m the best altitude that represents the mountain site? Please add also the most important megacities to the map to help estimating the influence of anthropogenic emissions.

We have added the vertical evolution of the trajectories. The beginning of southwesterly air masses traversed at lower heights relative to northerly air masses. Please refer to the Figure 2 (b). Heights of the HYSPLIT model in the study region (a spatial resolution of $0.5° \times 0.5°$) was averaged 500 m a.s.l, which was lower than height of the observed site (1,690 m a.s.l). Therefore, a height of 1,800 m a.s.l. (approximately 100 m above the observed site) was used as an endpoint in the model. Continental air masses crossed industrial areas where located in the Yangtze River Mid-Reaches city cluster (Figure 2a). The site was possibly affected by industrial emissions under the influence of continental air masses. Please refer to Lines 189-196 of the revised manuscript.

(a)

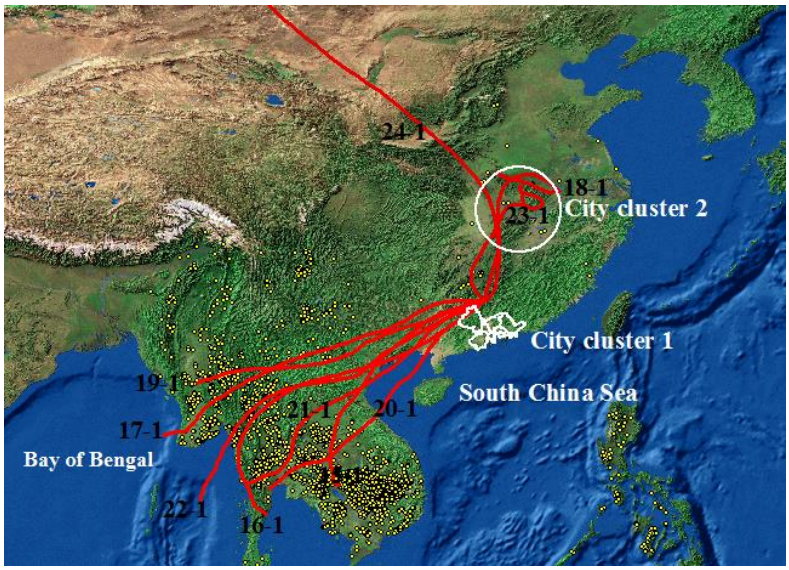

(b)

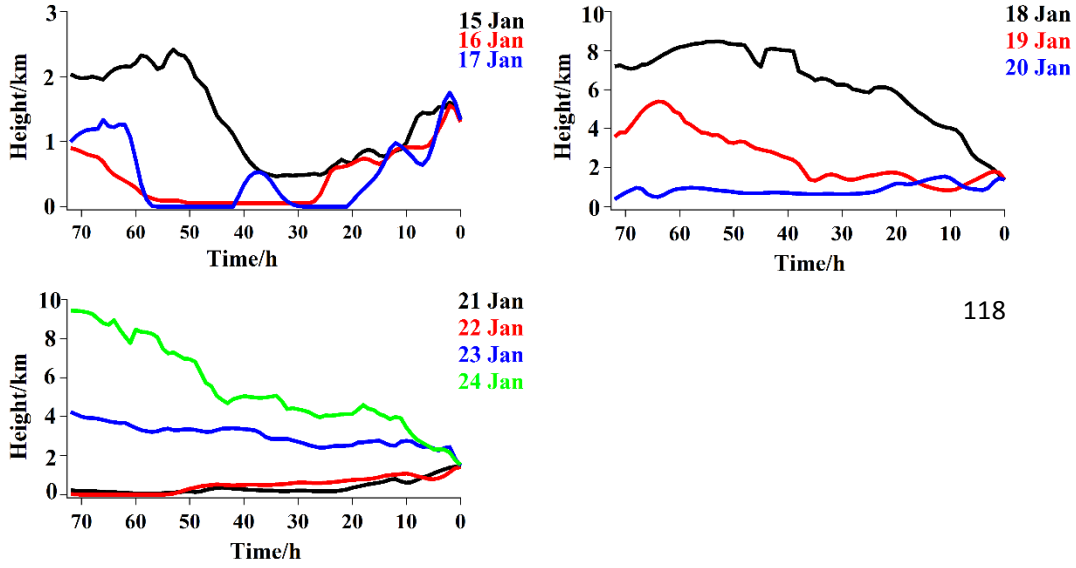

Figure 2: (a) HYSPLIT back trajectories (72 h) for air masses at 1,800 m during the whole sampling period. The white borders and circle refers to the Pearl River Delta (city cluster 1) and Yangtze River Mid-Reaches city cluster (city cluster 2), respectively. The yellow rots represent fire dots during the study periods. The fire dots are available at https://earthdata.nasa.gov/; (b) Heights (above model ground) of the air masses as a function of time.

Page 10, line 207: I suggest moving Figure S3 to the main paper.

Figure S3 has been moved to the main paper, please refer to Figure 4 in the revised manuscript.

Page 11, lines 221-222: But Roth et al. found a clear enhancement of amines in residues compared to the background aerosol (9% to about 2%).

We have added a comparison Nf of amine-containing particles between cloud residues and background aerosol reported by Roth et al., (2016). Please refer to Lines 265-267 of the revised manuscript.

Page 12, lines 235-237: I agree that dust is found more frequently in the coarse particle size range, but then I would expect to see an increase of the dust fraction in the residues with increasing diameter. This is not seen in Figure S3. Is the identification of dust reliable? What about the Fe-containing particles? They might be dust as well.

We agree with the comment. As a matter of fact, Nf of dust cloud residues generally increased with increasing diameter. Please refer to Lines 276-278 of the revised manuscript.

Approximately 16% of the Fe cloud residues contained Ca peak (m/z 40). Relatively weak Na and K peaks in the Fe particles possibly contributes to anthropogenic sources (Zhang et al., 2014), especially northern air mass across iron/steel industrial activities in Yangtze River Mid-Reaches city clusters (Figure 2). These might suggest that Fe cloud residues was likely to have come from mixed sources. Please refer to Lines 290-294 of the revised manuscript.

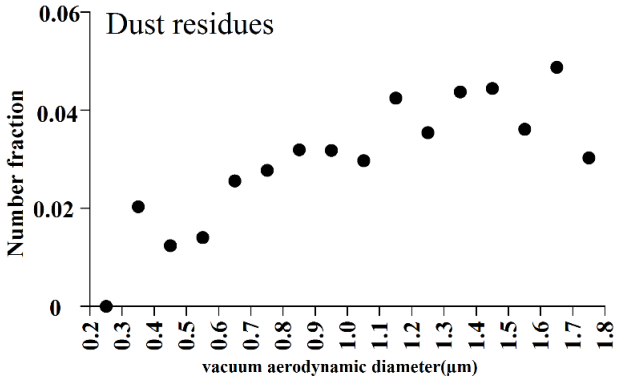

Page 12, lines 238-243: What could be the source of these Pb- and Fe-containing particles? See also comment above. Can the Fe-containing particles belong to the dust-type?

As mentioned above, the Fe cloud residues contain Ca peak (m/z 40, 16% by number) and relatively weak Na and K peaks, which possibly contributes to anthropogenic sources (Zhang et al., 2014), especially northern air mass across iron/steel industrial activities in Yangtze River Mid-Reaches city clusters (Figure 2). These might suggest that this particle type likely originated from mixed sources. Please refer to Lines 290-294 of the revised manuscript.

The Pb particles showed its typical ions at m/z 208Pb^+ and internally mixed with K and Cl. Previous studies found that K and Cl internally mixed with Pb particles have a possible origination of waste incineration (Zhang et al., 2009) or iron and steel facility (Tsai et al., 2007). Please refer to Lines 315-318 of the revised manuscript.

Page 12, lines 244-252: If these particles were from sea salt, they should contain chloride ions. That is hard to see in Figure 3. Are these Na-rich particles correlated with air masses coming from the ocean?

Na-rich particles result from varied sources of industrial emissions or sea salt particles and dry lake beds (Moffet et al. 2008). The Nf of the Na-rich cloud residues did not increase from continental (Northerly) air mass to maritime (southwesterly) air mass on 21 Jan (3.3% versus 2.4% by number). However, sea salt ion peak areas (m/z, 81/83$Na_2{}^{35}Cl$/$Na_2{}^{37}Cl$) were enhanced for Na-rich particles origination from maritime air mass relative to continental air mass (3.8 ±l2.4 times). Continental air masses crossed industrial areas where located in the Yangtze River Mid-Reaches city cluster (Figure 2). Industrial emissions was a possible contributor to Na-rich particles under the influence of continental air masses (Wang et al. 2016). This might suggests that the Na-rich particles were contributed by both the industrial emissions and sea salt. Therefore, under the influence of maritime air mass, the signals for sea salt contribution became stronger. Please refer to Lines 299-310 of the revised manuscript.

Page 13, line 259 and Figure 5: How do you distinguish between sulfuric acid and sulfate? Besides, spelling (sulfate, sulphuric acid) should be consistent ("f" or "ph").

Sulfate ion peak at m/z -97 HSO_4^- and sulfuric acid cluster ion peak at m/z -195 $[H(HSO_4)_2^-]$

were given in previous single particle studies (Pratt et al., 2009; Rehbein et al., 2011). "Sulphuric acid" has been replaced by "Sulfuric acid". Please refer to the caption of Figure 5.

Page 13, lines 265-267: What other forms of nitrate do you suggest to be present on the Na-rich and dust residues? What about uptake of nitric acid from the gas-phase by the cloud droplets? How certain is the identification of ammonium? Which peak was used?

The Na-rich and Dust types were mainly composed of alkaline ion peaks (m/z, $23Na^+$,$39K^+$ and $40Ca^+$) in the position mass spectra (Figure 3). This suggests that rather than NH_4NO_3, nitrate might exist in the form of $Ca(NO_3)_2$, $NaNO_3$ or KNO_3 in the dust and Na-rich cloud residues. Please refer to Lines 340-344 of the revised manuscript.

We agree with the comment. We have discussed the contribution of uptake of gas-phase HNO_3 to enhanced nitrate in the cloud residues and cited Schneider et al. (2017). Please refer to Lines 334-335 of the revised manuscript.

Generally, a NH_4^+ ion signal (m/z 18) was used for identification of ammonium in the analysis of single particle mass spectrometry (Pratt et al., 2009). Please refer to Line 338 of the revised manuscript.

Page 13, line 268-272: The stability of ammonium nitrate depends also on the humidity. In the book by Seinfeld and Pandis (2nd edition, Wiley and Sons, 2006, Chapter 10.4.3) it is shown that at 30% RH ammonium nitrate does not exist above 30 C. I would assume that the dry carrier gas in the evaporation section is below 30% RH. Thus, it may well be that NH4NO3 evaporates in your system.

We agree with the comment. We have clarified the artificial effect on ammonium nitrate in the cloud residues. Please refer to Lines 344-346 of the revised manuscript.

Page 13, lines 275-276: The sentences "The presence of abundant sulfate in aged EC cloud residues was considered to be a good CCN species before activation:" needs rephrasing. It is not clear to me what you want to say. Do you mean "aged EC particles mixed with sulfate are good CCN"?

The sentence has been changed to "aged EC particles mixed with sulfate are good CCN".

Please refer to Lines 350 of the revised manuscript.

Page 13, line 279: Ammonium will most likely play a key role in the form of ammonium sulfate or ammonium nitrate. In organic particles, amines may play that role (methylamines). Again: how do you identify ammonium and how do you distinguish between amines and ammonium?

We agree with the comment. Ammonium will most likely play a key role in the form of ammonium sulfate or ammonium nitrate in the OC and aged EC cloud residues (Zhang et al., 2017). Please refer to Lines 353-354 of the revised manuscript.

A NH_4^+ ion signal (m/z 18) was used for identification of ammonium. The existences of m/z 59 $N(CH_3)_3^+$ (trimethylamine,TMA) and related amine ion signals m/z 58$C_2H_5NHCH_2^+$ (diethylamine, DEA) and m/z 86$C_5H_{12}N^+$ (triethylamine, TEA)were used for identification of amines (Angelino et al., 2001). Please refer to Lines 254-257 and 338 of the revised manuscript.

Page 14, line 281 (and Figure 5): Why does oxalate nor correlate with OC?

Classification of the OC particles mainly based on intense organic carbon ion signals (e.g., m/z 27$C_2H_3^+$, 37C_3H^+, 43$C_2H_3O^+$ and 51$C_4H_3^+$). However, majority of oxalate-containing particles internally mixed with the K-rich type. Therefore, oxalate was classified to the K-rich type, probably contributed from biomass burning. Noted that K-rich could contain a large abundant of organics (Pratt et al. 2011), however, the signals of organics were covered by the potassium due to its high sensitive to the laser. Please refer to Lines 371-378 of the revised manuscript.

Page 14, lines 284-285: What do you mean by "enrichment of TMA in amine cloud residuals"? You observe that in 93% of those cloud residuals that are assigned to the "amine" type contain TMA. That is not surprising, more surprising is that it's not 100%. But that's inside the measurement uncertainties, to my opinion.

We have changed "enrichment of TMA in amine cloud residuals" to "presence of TMA in amine cloud residuals". Please refer to Lines 360-361 of the revised manuscript.

Amine family signals m/z 58$C_2H_5NHCH^{2+}$ and m/z 86$C_5H_{12}N^+$ were also selected to

identify amines (Angelino et al., 2001), leading to only 93% of the "amine" residues containing TMA. Particles that exist a peak signal m/z 58$C_2H_5NHCH_2^+$, were found to account for 99% of the Amine residues. Please refer to Lines 254-257 of the revised manuscript.

Page 14, lines 294-295: "This may result in 33% by number to the Amine residues containing oxalate." Please rephrase, not clear what you want to say.

We have rephrased this sentence to "it may facilitate the entrainment of oxalate (33% by number) in the Amine residues. ". Please refer to Lines 370-371 of the revised manuscript.

Page 14, line 298: What does "unscaled" mean? These are absolute particle numbers.

Considering that the SPAMS mainly detected in size range 0.2-2.0 μm and has size-dependent transmission efficiency. Detected particles were not corrected by a SMPS. Therefore, detected particles cannot represent real atmospheric particle level. "unscaled" has been changed to "detected particle counts". Please refer to Line 381 of the revised manuscript.

Page 14, lines 302-303: You say that the air masses change from northerly on 18 Jan to southwesterly on 19 Jan, but the particles remain similar from 17 Jan (around noon) to 20 Jan (noon). On the other hand, the change in particle types is very abrupt from cloud residuals to ambient on Jan 17.

Southwesterly wind flow on 19-20 Jan was too weak (~ 2.75 m s^{-1}) to dilute particles originated from northerly air masses (Figure 1). Additionally, high RH (90%) contour line at height 1,500 m (a.s.l.) gradually moved to north China from 19 to 20 Jan (Figure S5). These might lead to similar residual particle types observed from 19 Jan to 20 Jan, although the site encountered southwesterly cloudy air on 19-20 Jan (Figure 2). Please refer to Lines 400-404 of the revised manuscript.

Ambient RH showed an abrupt decrease from nearly 100% at 10:00 to 85% at 11:00 on 17 Jan (Figure 1). The entrained particles originated from northern air mass might have insufficient supersaturation to activate as cloud droplets. It leads to a very abrupt change in Nf of particle types from cloud residues to ambient particles on Jan 17. Please refer to Lines 382-390 of the revised manuscript.

Page 15, lines 322-325: Do verify the possible transport of biomass burning particles to the site, the vertical history of the trajectories is required.

We have added the vertical evolution of the trajectories. The beginning of trajectories traversed at low heights (about 0-2 km above model ground) of Southeast Asia, where abundant fire dots occurred. Please refer to the Figure 2 (b).

(a)

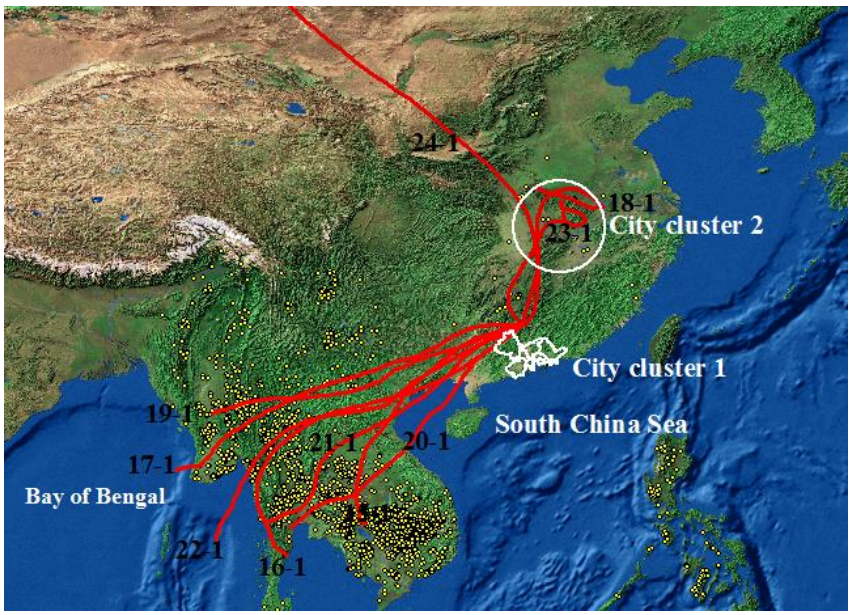

(b)

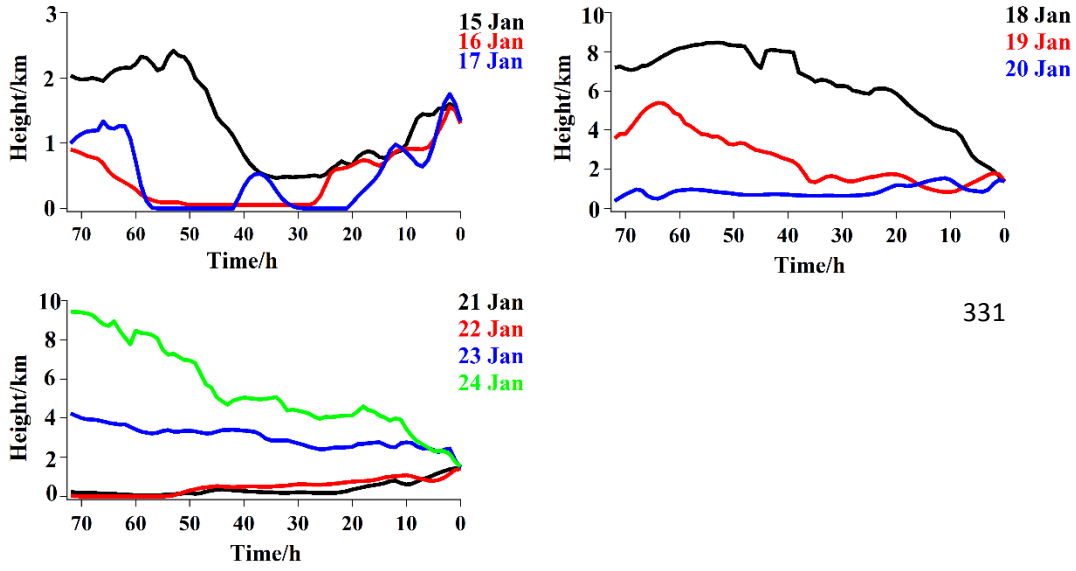

Figure 2: (a) HYSPLIT back trajectories (72 h) for air masses at 1,800 m during the whole sampling period. The white borders and circle refers to the Pearl River Delta (city cluster 1) and Yangtze River Mid-Reaches city clusters (city cluster 2), respectively. The yellow rots represent fire dots during the study periods. The fire dots are available at https://earthdata.nasa.gov/; (b) Heights (above model ground) of the air masses as a function of time.

Page 16, lines 337-229: "Note that after the activation of amine particles, the partitioning of the gas amine on cloud droplets may further contribute to the enhanced Amine cloud residues". That is true, but holds also for other species, as nitrate (HNO3) or water-soluble OC.

We have strengthened the important contribution of uptake of gaseous HNO_3 or water-soluble OC to cloud droplets. Please refer to Lines 334-335, 364-366 and 490-494 of the revised manuscript.

Section 3.5: Here I have a major concern: You report interstitial particles containing sulfate and nitrate in the size range between 200 and 1300 nm. It is very hard to believe (not to say impossible) that such large particles are not activated in a cloud.

Later (page 17, lines 366-368) you write " However, few studies have focused on this issue, in part because interstitial particles show a smaller size than that detected by single-particle mass spectrometry (Roth et al., 2016)." Since the SPAMS has a very similar lower detection size range as the ALABAMA used by my group in Roth et al., 2016), you can not expect that you detect non-activated interstitial particles which should be in the size range below 200 nm.
My suspicion is: The clouds became thinner, and entrainment of cloud-free air has mixed "normal" aerosol particles into the cloud. But such particles cannot be referred to as "interstitial". As long as you don't have cloud microphysics (number and size of cloud droplets) or at least liquid water content (Particle Volume Monitor) available, I would suggest to remove this chapter on interstitial particles.

The period of collecting interstitial particles on 22-23 Jan encountered initial mixing of northerly cloud-free air (dry and cold airstreams) and southwesterly cloudy air (moist airflows). The dry northern air mass might lower supersaturation, only larger particles could be activated. This might result in above 200 nm non-activated particles observed

here (Mertes et al., 2005; Kleinman et al., 2012; Hammer et al., 2014). To make it more accurate, we prefer to name "non-activated particles", rather than "interstitial particles". We have clarified them. Please refer to Lines 453-461 of the revised manuscript.

Page 17, line 358 / Table 1: I would prefer a graph with bars or pie charts. I also strongly recommend showing the SMPS size distributions from residues, ambient and interstitial. That might help to identify the issues with the large interstitial particles.

Table 1 was replaced by pie charts. Please refer to Figure 7 in the revised manuscript. The SMPS size distributions from residues, ambient and interstitial particle were provided in Figure S2.

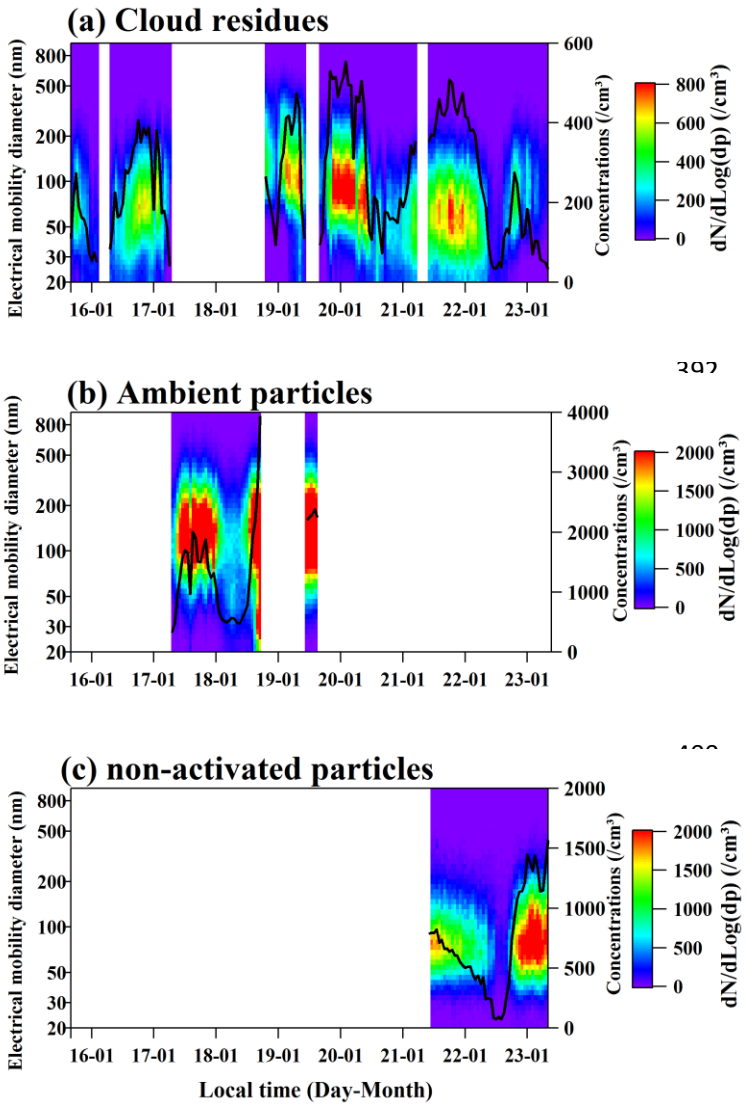

Figure S2: Size distribution (electrical mobility diameter 20-900 nm) of cloud residues (a),

ambient (b) and non-activated (c) particles were measured a scanning mobility particle sizer (SMPS). Black lines represent particles concentrations integrated by the SMPS. The data of cloud residual concentrations was corrected by enrichment factor of 5.25.

Page 18, lines 374-375 / Figure 7 & 8: How are the difference mass spectra of Figure 7 and 8 calculated? Is it ambient - residues and interstitial – residues? Or vice versa? How were the spectra normalized? Please explain.

We have provide the information in the captions of Figures 8 and 9 of the revised manuscript. Please refer to Lines 484-485 of the revised manuscript.

Figures 8: Mass spectral subtraction plot of the average mass spectrum corresponding to cloud residues minus ambient particles. Positive area peaks correspond to higher abundance in cloud residues, whereas negative area peaks show higher intensity in ambient particles.

Figure 9: Mass spectral subtraction plot of the average mass spectrum corresponding to cloud residues particles minus non-activated particles. Positive area peaks correspond to higher abundance in cloud residues, whereas negative area peaks show higher intensity in non-activated particles.

Page 18, lines 376-382: Why not? I drew the same conclusion as Hayden et al. (2008) in my 2017 paper (Schneider et al., 2017, please note the update from ACPD 2016 to ACP 2017). HNO3 uptake may not be the source of the particles but explains the high amount of nitrate found on many particles, also on the Na-rich and dust particles discussed above.

We agree with the comment. We have strengthened the contribution of uptake of gaseous HNO_3 to the enhanced nitrate in the cloud residues. We have update the citation of Schneider et al. (2017) from ACPD 2016 to ACP 2017. Please refer to Lines 334-335 and 490-494 of the revised manuscript.

Page 18, lines 384-386: I agree with that, but wouldn't that support the idea of uptake of HNO3 from the gas phase? If the nitrate content does not play the major role in the activation, but more nitrate is found in the residues, that's an argument for HNO3 uptake.

We agree with the comment. We have strengthened the contribution of uptake of gaseous HNO_3 to the enhanced nitrate in the cloud residues. Please refer to Lines 334-335 and 490-494 of the revised manuscript.

Page 18, lines 387-388: Can intensity simply be compared like this? What about size effects and matrix effects? But again, an explanation how Figures 7 and 8 were calculated might help here.

We agree with the comment. Size and matrix might affect the mass spectra of single particles. Such comparison has been perform in previous single particle studies (Moffet et al., 2008; Pratt et al., 2011). In addition to comparison of certain compound's intensity, its size distribution and number fractions of cloud residues was compared with ambient or non-activated particles, to discuss size effect. Please refer to Lines 487-492 and 504-505 of the revised manuscript.

Figure 8 and 9 show differences in average mass spectra for cloud residues versus ambient particles, as well as cloud residues versus non-activated particles, respectively. Intensity refers to peak area. Please refer to Lines 484-485 of the revised manuscript.

Figures 8: Mass spectral subtraction plot of the average mass spectrum corresponding to cloud residues minus ambient particles. Positive area peaks correspond to higher abundance in cloud residues, whereas negative area peaks show higher intensity in ambient particles.

Figure 9: Mass spectral subtraction plot of the average mass spectrum corresponding to cloud residues particles minus non-activated particles. Positive area peaks correspond to higher abundance in cloud residues, whereas negative area peaks show higher intensity in non-activated particles.

Page 18, lines 391-392: "Compared with interstitial particles, sulfate enhanced in the Fe cloud residues." I think an "is" is missing here.

We have changed "Compared with interstitial particles, sulfate enhanced in the Fe cloud residues." to "Compared with non-activated particles, sulfate was found to enhance in the Fe cloud residues.". Please refer to Lines 503-504 of the revised manuscript.

Page 19, lines 398-399: Better: "The in-cloud process has been reported to be an important pathway: : :"

We have changed accordingly. Please refer to Lines 510-511 of the revised manuscript.

Page 20, lines 421-422: The Jungfraujoch is a station located mostly in the free troposphere and in a remote region, so the biomass burning contribution can be expected to be lower than at other sites.

We agree with the comment. We have discussed less number fraction of biomass burning in the observed cloud residues at the Jungfraujoch station, where located mostly in the free troposphere and in a remote region. Please refer to Lines 251-253 of the revised manuscript.

Figures

Figure 3: Please improve resolution. Labels can't be read upon zooming in.

We have improved Figure 3 resolution. Please refer to the modified Figure 3. Average mass spectrum of Pb, OC and Other types have been moved to the supplemental information (Figure S4)

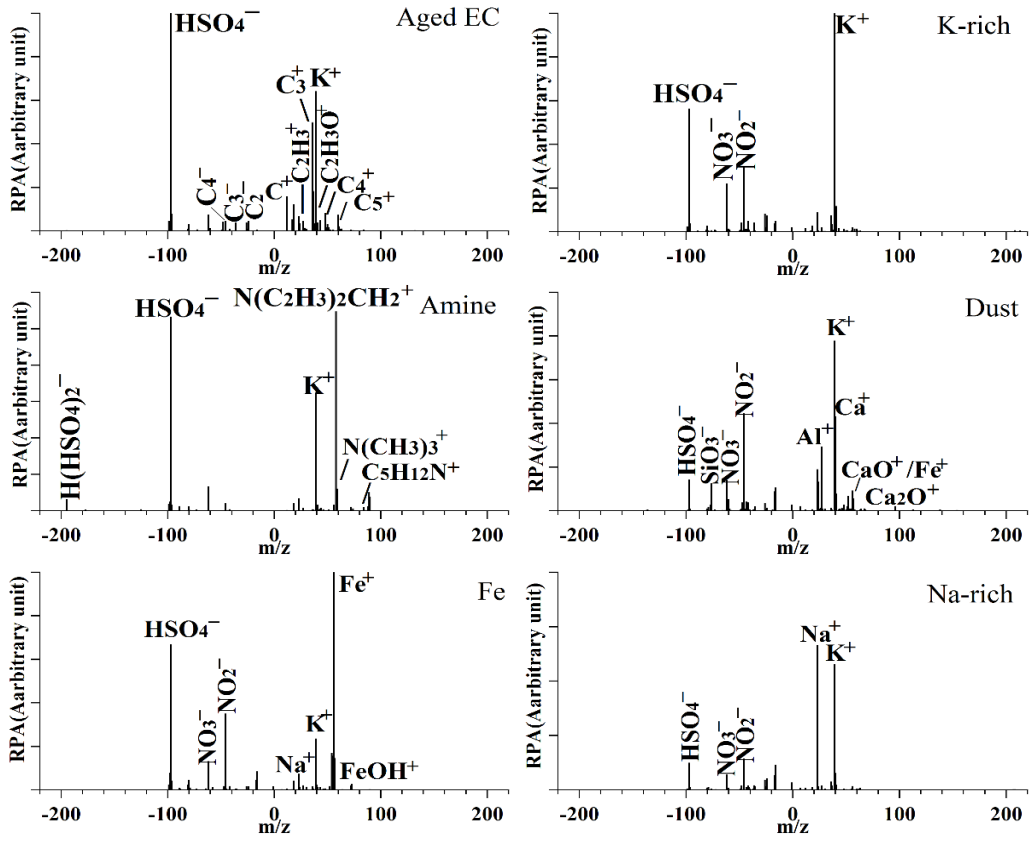

Figure 3: Averaged positive and negative mass spectra for the main 6 particle types (Aged EC, K-rich, Amine, Dust, Fe, Na-rich) of the sampled particles during the whole sampling period. RPA in the vertical axis refers to relative peak area. m/z in the horizontal axis represents mass-to-charge ratio.

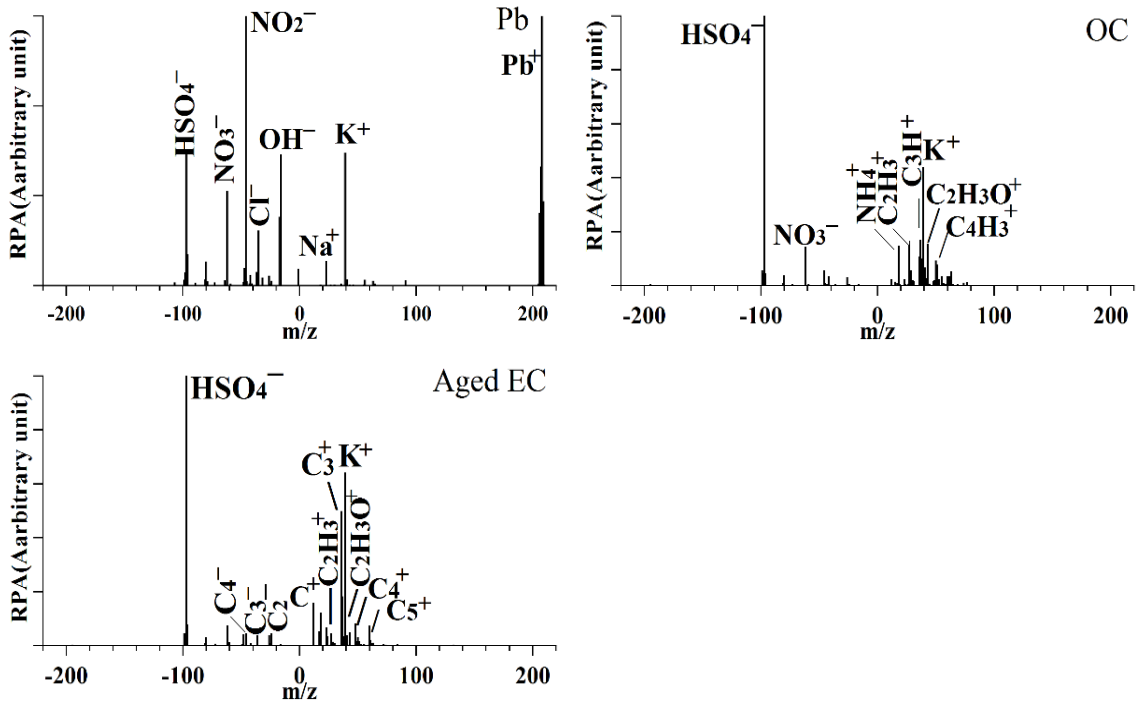

Figure S4: Averaged positive and negative mass spectra for Pb, OC and Other types of the sampled particles during the whole sampling period. RPA in the vertical axis refers to relative peak area. m/z in the horizontal axis represents mass-to-charge ratio.

Figure 6: The ambient particle time series (b) are broader than the corresponding gaps in (a). Please make the Figure broader. You can move the legend with the particle types to above or below the graphs, plus the legend is only needed once.

Ambient and cloud residues were collected at the same hour, which lead to ambient particle time series (b) broader than the corresponding gaps in (a). Figure 6 has been changed accordingly. Please refer to the modified Figure 6.

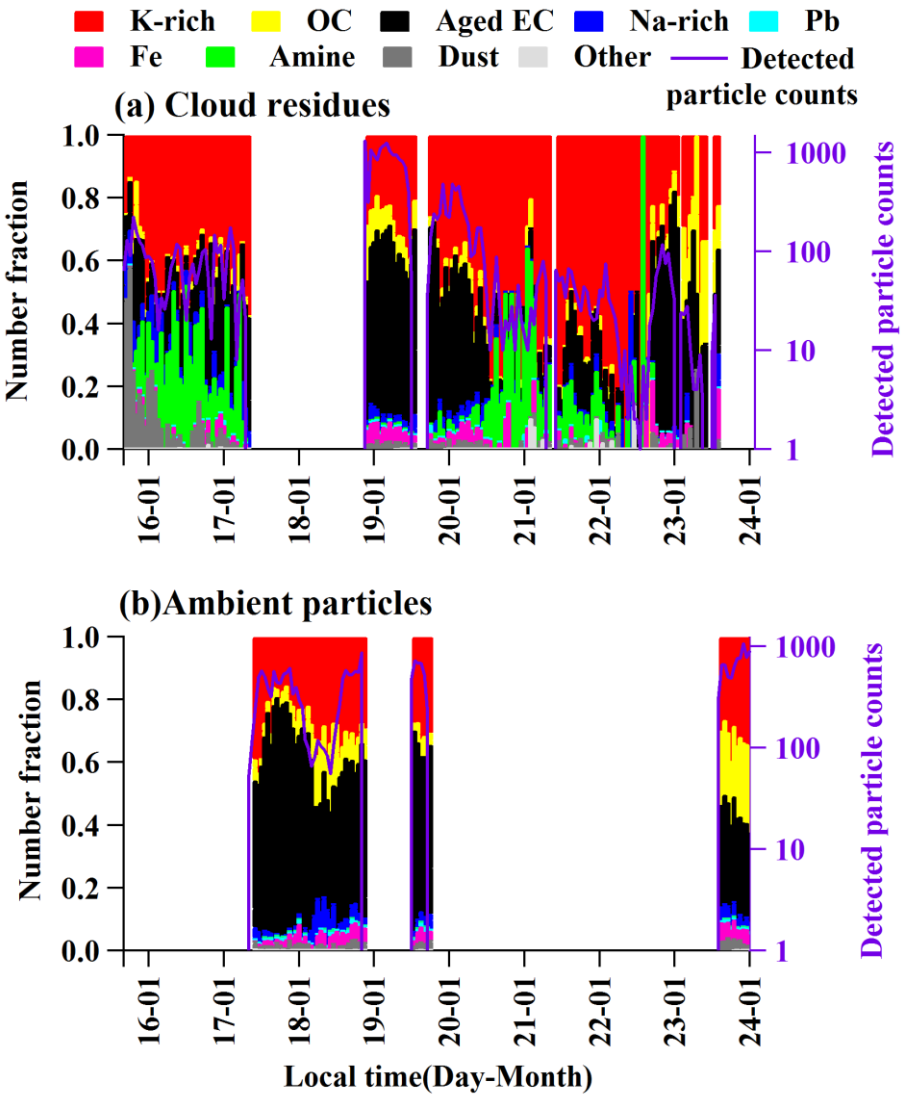

Figure 6: The hourly average variations in the cloud residual and ambient particles during the whole sampling period.

References:

Hammer, E., Gysel, M., Roberts, G.C., Elias, T., Hofer, J., Hoyle, C.R., Bukowiecki, N., Dupont, J.C., Burnet, F., Baltensperger, U. and Weingartner, E.: Size-dependent particle activation properties in fog during the ParisFog 2012/13 field campaign, Atmos. Chem. Phys., 14, 10517-10533, 2014.

Kleinman, L.I., Daum, P.H., Lee, Y.-N., Lewis, E.R., Sedlacek III, A., Senum, G., Springston, S., Wang, J., Hubbe, J. and Jayne, J.: Aerosol concentration and size distribution measured below, in, and above cloud from the DOE G-1 during VOCALS-Rex, Atmos. Chem. Phys., 12, 207-223, 2012.

Li, T., Wang Y., Zhou J., Wang T., Ding A., Nie W., Xue L., Wang X., and Wang W.: Evolution of trace

elements in the planetary boundary layer in southern China: Effects of dust storms and aerosol-cloud interactions, J. Geophys. Res. Atmos., 122, doi:10.1002/ 2016JD025541, 2017.

Lohmann, U., Stier, P., Hoose, C., Ferrachat, S., Kloster, S., Roeckner, E., Zhang, J.: Cloud microphysics and aerosol indirect effects in the global climate model ECHAM5-HAM, Atmos. Chem. Phys., 7, 3425-3446, 2007.

Mertes, S., Lehmann, K., Nowak, A., Massling, A. and Wiedensohler, A.: Link between aerosol hygroscopic growth and dropletactivation observed for hill-capped clouds at connected flow conditions during FEBUKO, Atmos. Environ., 39, 4247-4256, 2005.

Moffet, R.C., Foy, B. d., Molina, L. a., Molina, M., and Prather, K.: Measurement of ambient aerosols in northern Mexico City by single particle mass spectrometry, Atmos. Chem. Phys., 8, 4499-4516, doi:10.5194/acp-8-4499-2008, 2008.

Pratt, K. A., Heymsfield, A. J., Twohy, C. H., Murphy, S. M., DeMott, P. J., Hudson, J. G., Subramanian, R., Wang, Z., Seinfeld, J. H., and Prather, K. A.: In Situ Chemical Characterization of Aged Biomass-Burning Aerosols Impacting Cold Wave Clouds, J. Atmos. Sci., 67, 2451-2468, doi:10.1175/2010jas3330.1, 2010a.

Pratt, K.A., Murphy, S., Subramanian, R., DeMott, P., Kok, G., Campos, T., Rogers, D., Prenni, A., Heymsfield, A., Seinfeld, J.: Flight-based chemical characterization of biomass burning aerosols within two prescribed burn smoke plumes, Atmos. Chem. Phys., 11, 12549-12565, doi:10.5194/acp-11-12549-2011, 2011.

Rosenfeld, D., Lohmann, U., Raga, G.B., O'Dowd, C.D., Kulmala, M., Fuzzi, S., Reissell, A., Andreae, M.O.: Flood or drought: how do aerosols affect precipitation? Science, 321, 1309-1313, doi: 10.1126/science.1160606, 2008.

Roth, A., Schneider, J., Klimach, T., Mertes, S., van Pinxteren, D., Herrmann, H., and Borrmann, S.: Aerosol properties, source identification, and cloud processing in orographic clouds measured by single particle mass spectrometry on a central European mountain site during HCCT-2010, Atmos. Chem. Phys., 16, 505-524, doi:10.5194/acp-16-505-2016, 2016.

Schneider, J., Mertes, S., van Pinxteren, D., Herrmann, H., and Borrmann, S.: Uptake of nitric acid, ammonia, and organics in orographic clouds: Mass spectrometric analyses of droplet residual and interstitial aerosol particles, Atmos. Chem. Phys., 17, 1571-1593, doi:10.5194/acp-17-1571-2017, 2017.

Seinfeld, J.H., Bretherton, C., Carslaw, K.S., Coe, H., DeMott, P.J., Dunlea, E.J., Feingold, G., Ghan, S., Guenther, A.B., Kahn, R.: Improving our fundamental understanding of the role of aerosol-cloud interactions in the climate system. Proc. Natl. Acad. Sci. USA, 113, 5781-5790, doi: 10.1073/pnas.1514043113, 2016.

Sorooshian, A., Ng, N. L., Chan, A. W. H., Feingold, G., Flagan, R. C., and Seinfeld, J. H.: Particulate organic acids and overall water-soluble aerosol composition measurements from the 2006 Gulf of

Mexico Atmospheric Composition and Climate Study (GoMACCS), J. Geophys. Res. Atmos., 112(D13), doi:10.1029/2007JD008537, 2007a.

Stier, P., Feichter, J., Kinne, S., Kloster, S., Vignati, E., Wilson, J., Ganzeveld, L., Tegen, I., Werner, M., Balkanski, Y.: The aerosol-climate model ECHAM5-HAM. Atmos. Chem. Phys., 5, 1125-1156. 2005.

Tang, M., Cziczo, D. J., and Grassian, V. H.: Interactions of Water with Mineral Dust Aerosol: Water Adsorption, Hygroscopicity, Cloud Condensation, and Ice Nucleation, Chem. Rev., doi:10.1021/acs.chemrev.5b00529, 2016.

Tsai, J.H., Lin, K.H., Chen, C.Y., Ding, J.Y., Choa, C.G. and Chiang, H.L.: Chemical constituents in particulate emissions from an integrated iron and steel facility, J. Hazard. Mater., 147, 111-119. 2007.

Wang, H., An, J., Shen, L., Zhu, B., Xia, L., Duan, Q. and Zou, J.: Mixing state of ambient aerosols in Nanjing city by single particle mass spectrometry, Atmos. Environ., 132, 123-132, 2016.

Zhang, G., Bi, X., Lou, S., Li, L., Wang, H., Wang, X., Zhou, Z., Sheng, G., Fu, J. and Chen, C.: Source and mixing state of iron-containing particles in Shanghai by individual particle analysis, Chemosphere, 95, 9-16, 2014.

Zhang, G., Lin, Q., Peng, L., Bi, X., Lei, M., Chen, D., Brechtel, F.J., Chen, X., Yan, W.,Wang, X., Peng, P., Sheng., G., Zhou, Z.: Single particle mixing state and cloud scavenging of black carbon at a high-altitude mountain site in south China, J. Geophys. Res. Atmos. Submitted, 2017.

Zhang, Y.P., Wang, X.F., Chen, H., Yang, X., Chen, J.M. and Allen, J.O.: Source apportionment of lead-containing aerosol particles in Shanghai using single particle mass spectrometry, Chemosphere, 74, 501-507, 2009.

In situ chemical composition measurement of individual cloud residue particles at a mountain site, South China

Qinhao Lin[1,2], Guohua Zhang[1], Long Peng[1,2], Xinhui Bi[1,*], Xinming Wang[1], Fred J. Brechtel[3], Mei Li[4], Duohong Chen[5], Ping'an Peng[1], Guoying Sheng[1], Zhen Zhou[4]

[1] State Key Laboratory of Organic Geochemistry and Guangdong Key Laboratory of Environmental Protection and Resources Utilization, Guangzhou Institute of Geochemistry, Chinese Academy of Sciences, Guangzhou, 510640, PR China

[2] University of Chinese Academy of Sciences, Beijing, 100049, PR China

[3] Brechtel Manufacturing Inc., Hayward, 94544, California, USA

[4] Atmospheric Environment Institute of Safety and Pollution Control, Jinan University, Guangzhou 510632, PR China

[5] State Environmental Protection Key Laboratory of Regional Air Quality Monitoring, Guangdong Environmental Monitoring Center, Guangzhou 510308, PR China

* Correspondence to: Xinhui Bi (bixh@gig.ac.cn)

Tel.: +86-20-85290195

Highlights

1. EC-containing particles comprised the largest fraction of the total cloud residues (49.3% by number), with dominating size 0.2-1.0 μm.

2. Amine particles represented 0.2% to 15.1% by number of the total cloud residues dependent on the air mass history, with dominating size 0.7-1.9 μm.

3. Higher fraction, intensity (average ion peak area) and larger size of nitrate-containing particles were found in the cloud residues relative to the ambient particles.

Abstract

To estimate how atmospheric aerosol particles interact with chemical composition of cloud droplets, a ground-based counterflow virtual impactor (GCVI) coupled with a real-time single-particle aerosol mass spectrometer (SPAMS) was used to assess the chemical composition and mixing state of individual cloud residue particles in the Nanling Mountain Range (1,690 m a.s.l.), South China, in Jan 2016. The cloud residues were classified into nine particle types: Aged elemental carbon (EC), Potassium-rich (K-rich), Amine, Dust, Pb, Fe, Organic carbon (OC), Sodium-rich (Na-rich) and Other. The largest fraction of the total cloud residues was the aged EC type (49.3% by number), followed by the K-rich type (33.9% by number). Abundant aged EC cloud residues that internally mixed with inorganic salts were found in air masses from northerly polluted areas. The number fraction (Nf) of the K-rich cloud residues increased within southwesterly air masses from fire activities in Southeast Asia. In addition, the Amine particles increased from 0.2% to 15.1% by number to the total cloud residues, when air masses changed from northerly polluted areas to southwesterly ocean and livestock areas. The Dust, Fe, Pb, Na-rich and OC particles had a low contribution (0.5-4.1% by number) to the total cloud residues. Higher fraction of nitrate (88-89% by number) was found in the Dust and Na-rich cloud residues relative to sulfate (41-42%) and ammonium (15-23%). Higher fraction, intensity (average ion peak area) and larger size of nitrate-containing particles were found in the cloud residues relative to the ambient particles. To our knowledge, this study is the first report on in situ observation of the chemical composition and mixing state of individual cloud residue particles in China. This study increases our understanding of the impacts of aerosols on cloud droplets in a remote area of China.

Keywords: GCVI, SPAMS, cloud residues, mixing state, South China

1 Introduction

Aerosol-cloud interactions influence the thermodynamic and radiation balance of the atmosphere (IPCC, Boucher et al., 2013). Anthropogenic particles can increase number concentration of small cloud droplets, in turn, affect reflectivity and life time of clouds (Stier et al., 2005; Lohmann et al., 2007; Rosenfeld et al., 2008). In-situ cloud chemical measurements show varied chemical composition of cloud water or residues at various regions (Sorooshian et al., 2007a; Roth et al., 2016; Li et al., 2017). Although a large number of aerosol/cloud studies over the past 20 years, the uncertainty for evaluating radiative forcing due to aerosol-cloud interactions has not been reduced (Seinfeld. et al., 2016). Therefore, it is crucial to assess how atmospheric aerosol particles contribute and interact with cloud droplets.

The formation of cloud condensation nuclei (CCN) is dependent on the size and chemical composition of atmospheric aerosol particles at a given supersaturation (McFiggans et al., 2006). A change in the chemical composition of atmospheric aerosol particles during atmospheric aging processes can strongly alter their CCN ability. The presence of hydrophobic surface films lowers the CCN ability of atmospheric aerosol particles (Andreae and Rosenfeld, 2008). Elemental carbon (EC) particles, normally considered insoluble, show high CCN activity after mixing with sulfuric acid (Zhang et al., 2008). However, sulfate and nitrate, which are generally regarded as soluble materials, were found in particles ranging from high to low hygroscopicity (Herich et al., 2008).

Furthermore, several cloud measurements have pointed to a lower number fraction (Nf) or mass fraction of sulfate-containing particles in cloud droplets relative to ambient or interstitial particles (Drewnick et al., 2007; Twohy and Anderson, 2008). On the contrary, other studies have reported a larger Nf of sulfate-containing particles in cloud droplets (Zelenyuk et al., 2010; Roth et al., 2016). These discrepancies suggest that the influence of the mixing state of atmospheric aerosol particles on CCN activity remains unclear.

The combined technique of a counterflow virtual impactor (CVI) and Aerosol Mass Spectrometer (AMS) or single-particle measurement is widely used to characterize the chemical composition and mixing state of cloud/fog droplet residue particles. These studies were mainly conducted in North America including Wyoming (Pratt et al., 2010a), Ohio (Hayden et al., 2008), Oklahoma (Berg et al., 2009), Florida (Cziczo et al., 2004; Twohy et al., 2005), California (Coggon et al., 2014), Europe including Schmücke (Roth et al., 2016; Schneider et al., 2017), Jungfraujoch (Kamphus et al., 2010), Åreskutan (Drewnick et al., 2007), Scandinavia (Targino et al., 2006), Arctic (Zelenyuk et al., 2010), Central America (Cziczo et al., 2013), West Africa (Matsuki et al., 2010) and Oceans (Twohy and Anderson 2008; Twohy et al., 2009; Shingler et al., 2012). Over the past three decades, China has undergone rapid economic growth accompanied by increased aerosol emissions. Scientists have worked to increase our understanding of an emissions inventory and the temporal and spatial variation of atmospheric aerosols in China (Zhang et al., 2012b). However, few studies employ direct observation of the chemical composition and mixing state of cloud/fog droplets. Li et al. (2011b) used transmission electron microscopy to obtain mixing state of single ambient particle during cloud events at Mt. Tai in northern China. Their result showed that sulfate-related salts dominated in large particle. Bi et al.

(2016) used a ground-counterflow virtual impactor (GCVI) coupled with a real-time single particle aerosol mass spectrometer (SPAMS) to explore the chemical composition and mixing state of single fog residue particles in an urban area of South China at ground level. They found abundant anthropogenic emitted particles including soot or element carbon (EC) in fog residues.

Here, we present a study on the chemical composition and mixing state of individual cloud residue particles at a mountain site of South China. The same experimental methods of Bi et al. (2016) were used in this study on the summit of South China's Nanling mountain region. The size distribution, chemical composition and mixing state of cloud residues during cloud events are discussed. Moreover, the chemical compositions of ambient and non-activated particles were also compared with the cloud residues. The aim of this study is to assess the potential effects of anthropogenic aerosols from regional transportation on cloud formation and to investigate the dominant particle types in cloud droplets at a mountain site in South China.

2 Experimental

2.1 Measurement site

Measurements were carried out 15-26 Jan, 2016. The sampling site was located in the Nanling Background Station (112 °53' 56" E, 24° 41' 56" N, 1,690 m a.s.l.) at the National Air Pollution Monitoring System in South China (Figure S1). This station is 200 km north of the metropolitan city Guangzhou and 350 km north of the South China Sea. This site is also surrounded by a national park forest (273 km^2) where there are hardly any emissions from anthropogenic activities. However, during the winter monsoon period, air pollution

from northern China moves south to the southern coastal region and crosses the study region (Lee et al., 2005).

2.2 Instrumentation

In this study, a GCVI inlet system (GCVI Model 1205, Brechtel Mfg. Inc.) was used to sample cloud droplets with a diameter greater than 8 μm. Ambient temperature on average was 6.9 ℃ (ranging from -7.2 to 11.4 ℃) during cloud events in this study. Therefore, the clouds here consisted of liquid droplets only. Measurement of drop size spectrum in this region performed during winter of 1999-2001 shows that size of cloud droplets ranged from 4 to 25 μm, with average size of 10 μm and a corresponding liquid water content of 0.11-0.15 g m^{-3} (Deng et al., 2007). Some studies in other locations also showed an average size at ~10 μm (Freud et al., 2008; Shingler et al., 2012). Therefore, it is reasonable to select a cut size at 8 μm for cloud droplets in the present study. The sampled cloud droplets were passed through an evaporation chamber (air flow temperature at 40 ℃), where the associated water was removed and the dry residue particles (with the air flow RH lower than 30%), considered as CCN, remained. The particle transmission efficiency of the cut size (8 μm) was 50% (Shingler et al., 2012). The enrichment factor of the particles collected by the GCVI inlet was estimated to be 5.25 based on theoretical calculation (Shingler et al., 2012). Ambient particles were collected through an ambient inlet with a cut-off aerodynamic diameter (d_a) of 2.5 μm when no cloud events were present. Additionally, non-activated particles were sampled through the ambient inlet during the cloud events. The cloud droplet residues, ambient or non-activated particles were subsequently analyzed by a suite of aerosol measurement devices, including a SPAMS (Hexin Analytical

Instrument Co., Ltd., Guangzhou, China), a scanning mobility particle sizer (SMPS) (MSP Cooperation) and an aethalometer (AE-33, Magee Scientific Inc.). Detailed information and parameter settings regarding the GCVI operation can be found in the work of Bi et al. (2016).

A detailed operational principle of the SPAMS has been described elsewhere (Li et al., 2011a). Briefly, aerosol particles are drawn into SPAMS through a critical orifice. The particles are focused and aerodynamically sized by two continuous diode Nd:YAG laser beams (532 nm). The particles are subsequently desorbed/ionized by a pulsed laser (266 nm) triggered exactly based on the velocity of the specific particle. The positive and negative ions generated are recorded with the corresponding size of each singe particle. Polystyrene latex spheres (Nanosphere Size Standards, Duke Scientific Corp., Palo Alto) of 0.2-2.0 μm in diameter were used to calibrate the sizes of the detected particles on the mountain top station. The ambient pressure was 830 hPa (826-842 hPa) during the measurements and during the calibration. Particles measured by SPAMS mostly fell within the size range of d_{va} 0.2-2.0 μm (Li et al., 2011a).

2.3 Definition of cloud events

To reliably identify the presence of cloud events, an upper-limit visibility threshold of 5 km and a lower-limit relative humidity (RH) threshold of 95% were set in the GCVI software (Bi et al., 2016). Three long-time cloud events occurred during the periods of 16:00 (local time) 15 Jan - 07:00 17 Jan (cloud I), 20:00 18 Jan - 12:00 19 Jan (cloud II) and 17:00 19 Jan - 13:00 23 Jan (cloud III), as marked in Figure 1. In addition, a cloud event occurred at 14:40 - 15:00 on 17 Jan, but we did not complete an analysis due to the

short duration of this cloud event. The measured cloud residual concentration was integrated by a SMPS and was divided by 5.25 (enrichment factor of CVI). The corrected cloud residual concentrations on average were 218 cm^{-3}, 284 cm^{-3} and 272 cm^{-3} for cloud I, cloud II and cloud III, respectively (Figure S2). Note that during cloud events, ambient RH was close to 100%, as illustrated in Figure 1. Low level of PM2.5 (~ 12.7 μg m^{-3}) excludes the influence of hazy days. A rainfall detector of the GCVI system was also used to exclude rain droplet contamination. When cloud events occurred without precipitation, sampling was automatically triggered by the GCVI control software.

2.4 Particle classification

During the study period, a total of 73996 sampled particles including 49322 ambient, 23611 cloud residues and 1063 non-activated particles with bipolar mass spectra were chemically analyzed in the size range of d_{va} 0.2-1.9 μm. The sampled particles were first classified into 101 clusters using an Adaptive Resonance Theory neural network (ART-2a) with a vigilance factor of 0.75, a learning rate of 0.05, and 20 iterations (Song et al., 1999). By manually combining similar clusters, aged EC, Potassium-rich (K-rich), Amine, Dust, Fe, Pb, Organic carbon (OC), and Sodium-rich (Na-rich), eight major particle types with distinct chemical patterns were obtained, which represented ~99.9% of the population of the detected particles. The remaining particles were grouped together as "Other". Assuming that number of individual particles follows Poisson distribution, standard errors for number fraction of particle type were estimated (Pratt et al., 2010a).

3 Results and discussion

3.1 Back trajectories and meteorological conditions

Back trajectories in this study were calculated using the Hybrid Single Particle Lagrangian Integrated Trajectory (HYSPLIT Model). Heights of the HYSPLIT model in the study region (a spatial resolution of 0.5 ° × 0.5 °) is averaged 500 m a.s.l., lower than height of the observed site (1,690 m a.s.l.). Therefore, a height of 1,800 m a.s.l. (approximately 100 m above the observed site) was chosen as an endpoint in the model. During the study period, the station was mainly affected by southwesterly or northerly air masses (Figure 2). In addition, the beginning of southwesterly air masses traversed at lower heights relative to northerly air masses (Figure 2). The southwesterly air masses, accompanied by warm and moist airflows, occurred during 15-17 and 20-21 Jan, which promoted cloud formation (Figure 1). Conversely, the northerly air masses, associated with cool and dry airstreams, occurred during 18 and 23-24 Jan and led to a decrease in temperature and relative humidity. Note that on 18-19 and 22-23 Jan, the air mass encountered initial mixing of northerly cloud-free air and southwesterly cloudy air. Entrained of nuclei particles originated from northern air mass would be activated to become cloud droplets (Sect. 3.4). On the other hand, entrainment of non-activated particles originated from northern air mass has also mixed into the cloud (Sect. 3.5).

Meteorological conditions were unstable, with high southwesterly flow (~ 6.5 m s^{-1}) during 15-17 and 20-22 Jan (Figure 1). The level of $PM_{2.5}$ remained low with a value of approximately 3 μg m^{-3} for this time period. A high level of $PM_{2.5}$ (~20 μg m^{-3}) was observed during 18 Jan when the northerly flow dominated. Similarly, the average $PM_{2.5}$ value reached 24 μg m^{-3} during 24 Jan when the local northerly and southwesterly flows occurred alternately. However, the particles still originated from northerly air masses for

this period (Figure 2). During 23-24 Jan, a big freeze associated with a violent northerly flow and a wind speed that exceeded the upper-limit speed (~12 m/s) of a wind speed sensor resulted in a sharp decrease in temperature (Figure 1).

3.2 The chemical characterization of cloud droplet residues

Figure 3 shows the average positive and negative mass spectra of main six particle types. The aged EC particles were identified by EC cluster ions (e.g., m/z $\pm 12C^{+/-}$, $\pm 36C_3^{+/-}$, $\pm 48C_4^{+/-}$, $\pm 60C_5^{+/-}$, …) and a strong K^+ ion signal (m/z $39K^+$) as well as a sulfate ion signal (m/z $-97HSO_4^-$), and minor organic markers (m/z $27C_2H_3^+$, $43C_2H_3O^+$) (Moffet and Prather, 2009). EC particles mainly originated from combustion processes (Bond et al., 2013). Strong K^+ ion signal observed here, it is likely that the aged EC particles in part are from biomass burning (Bi et al. 2011). The aged EC particle type was the largest fraction (49.3% by number) of the the total cloud residues (Figure S3). In addition, Nf of the aged EC residues significantly decreased from 54.1% in the size range of 0.2-1.0 μm to 19.2% in the size range of 1.1-1.9 μm (Figure 4). Note that the chemical composition of cloud residues is dependent on the particle size (Roth et al., 2016), and the number reported for each particle type might suffer the bias from size-dependent transmission efficiency (Qin et al., 2006). The relative fraction of cloud residues in 100 nm size interval is presented to minimize the influence of size-dependent transmission efficiency of single particle mass spectrometry (Roth et al., 2016).

The K-rich particles exhibited the highest peak at m/z $39K^+$, mainly combined with sulfate and nitrate (m/z $-46NO_2^-$, $-62NO_3^-$). The K-rich particles presumably result from biomass/biofuel burning source (Moffet et al., 2008; Pratt et al. 2011; Zhang et al., 2013).

Aged time 81-88 min of biomass burning particles show increase in the mass fractions of ammonium, sulfate, and nitrate (Pratt et al. 2011). In this study, the K-rich particles would be expected to experience aged process due to strong sulfate and nitrate signals (Hudson et al. 2004; Pratt et al. 2011). Aged biomass burning particles can participate in cloud droplets formation and show an effective CCN activity (Pratt et al. 2010a). The K-rich particle type, the second largest contributor, accounted for 33.9% by number of the the total cloud residues (Figure S3).

The abundant aged soot/EC and biomass burning particles were often detected in cloud residues (Pratt et al., 2010a; Roth et al., 2016). The contribution of local anthropogenic origins to aged soot and/or biomass burning particles in cloud/fog residues has been reported in Schmücke (Roth et al., 2016) and Guangzhou city (Bi et al., 2016). At the North Slope of Alaska, the measurement of biomass burning particles in cloud residues mainly resulted from Asia sources (Zelenyuk et al., 2010). Similarly, majority of aged EC and K-rich cloud residues observed here are expected to originate from long-range transportation due to insignificant sources of local anthropogenic emissions or fire dots. At the Jungfraujoch station (3,580 m a.s.l.) in Europe, the K-rich (biomass burning) particles was only found to contribute 3% of the cloud droplets and the aged EC cloud residue was insignificant (<1% by number) (Kamphus et al., 2010). The Jungfraujoch is a station where located mostly in the free troposphere and in a remote region, so the biomass burning contribution can be expected to be lower than at other sites.

The Amine particles were characterized by related amine ion signals at m/z 58$C_2H_5NHCH_2^+$ (diethylamine, DEA), 59$N(CH_3)_3^+$ (trimethylamine, TMA) and 86$C_5H_{12}N^+$ (triethylamine, TEA) (Angelino et al., 2001; Moffet et al., 2008; Pratt and

Prather, 2010). Note that amine peaks would be enhanced when using a 266 nm ionization laser and that the amines themselves may not comprise the majority of the particle mass (Pratt et al., 2009). This particle type also contained sulfuric acid ion signals at m/z -195$H(HSO_4)_2^-$, indicative of acidic particles (Rehbein et al., 2011). The Amine particles represented 3.8% by number of the total cloud residues (Figure S3). Higher Nf of the Amine residues was detected in size range from 0.7 to 1.9 μm relative to size range from 0.2 to 0.6 μm (16.7% versus 0.4%), as shown in Figure 4. Aqueous reaction improving the participation of amine has been observed in Guangzhou (Zhang et al., 2012a) and Southern Ontario (Rehbein et al., 2011). A recent study also shows a clear enhancement of amine-containing particles in cloud residues compared to the ambient particles (9% versus 2% by number) (Roth et al., 2016). It indicates a preferential formation of amine in cloud. However, this possibility was not supported by the observations of Bi et al. (2016), who did not detect amine-containing particles in fog residues. In this study, the Nf of the Amine particles varied from 0.2% to 15.1% of the total cloud residues dependent on air mass history (see Sect. 3.4).

The Dust particles presented significant ions at m/z $40Ca^+$, $56CaO^+/Fe^+$, $96Ca_2O^+$ and -$76SiO_3^-$. Internal mixing with sulfate and nitrate in the Dust particle is expect to act as CCN (Twohy and Anderson 2008; Twohy et al., 2009; Matsuki et al., 2010), despite sulfate and nitrate partly contribution from in-cloud production. This type contributed 2.9% by number of the total cloud residues (Figure S3). A slightly increase in Nf of the Dust residues was observed in size range above 0.5 μm relative to below 0.5 μm (3.0% versus 1.0%). At Mt. Tai in northern China, a high concentration of Ca^{2+} in cloud/fog water was mainly attributed to a sandstorm event during spring season (Wang et al., 2011). At Mt.

Heng in southern China, abundant crust-related elements (e.g., Al) observed in cloud water is due to Asian dust storms occurred on March-May (Li et al., 2017). Based on the backward trajectory, the site was less affected by sandstorm source in northwestern China during cloud events. Local dust emission by anthropogenic-disturbing soils or removing vegetation cover can be excluded as a result of forest protection. Additionally, dust residues may occupied larger CCN (Tang et al., 2016), which cannot be detected by the SPAMS. Therefore, a low fraction (2.9% by number) of dust cloud residue is reasonable in the present study.

The Fe particles had its typical ions at m/z 56Fe^+ and internally mixed with sulfate and nitrate. The Fe particle type made up 4.1% by number of the total cloud residues. Approximately 16% of the Fe cloud residues contained Ca^+ peak (m/z 40). Relatively weak Na^+ and K^+ peaks in the Fe particles possibly contributes to anthropogenic sources (Zhang et al., 2014), especially northern air mass across iron/steel industrial activities in Yangtze River Mid-Reaches city clusters (Figure 2). These might suggest that the Fe residues was likely to have come from mixed sources. The presence of Fe in the cloud droplets play an important role in aqueous-phase SO_2 catalytic oxidation in cloud processing (Harris et al., 2013), thus accelerating the sulfate content of Fe-containing particles in cloud processing.

The Na-rich particles were mainly composed of ion peaks at m/z 23Na^+ and 39K^+ in the positive mass spectra, and nitrate and sulfate species in the negative mass spectra. The Na-rich particle type made up 3.0% by number of the total cloud residues. Na-rich particles were resulted from varied sources including industrial emissions, sea salt or dry lake beds (Moffet et al. 2008). The Nf of the Na-rich cloud residues did not increase from continental (Northerly) air mass to maritime (southwesterly) air mass on 21 Jan (3.3% versus 2.4% by

number). However, related sea salt ion peak area (m/z, 81/83 $Na_2{}^{35}Cl/Na_2{}^{37}Cl$) were enhanced for Na-rich particles origination from maritime air mass relative to continental air mass (3.8 ±2.4 times). Continental air masses crossed industrial areas where located in the Yangtze River Mid-Reaches city cluster (Figure 2). Industrial emissions was a possible contributor to Na-rich particles under the influence of continental air masses (Wang et al. 2016). This might suggests that the Na-rich particles were contributed from both the industrial emissions and sea salt. Therefore, under the influence of maritime air mass, the signals for sea salt contribution became obvious.

The OC, Pb and Other particle types contributed 0.1-2.3% by number to the total cloud residues (Figure S3). Their average mass spectra can be found in Figure S4. The OC particles presented dominant intense OC signals (e.g., m/z $27C_2H_3^+$, $37C_3H^+$, $43C_2H_3O^+$ and $51C_4H_3^+$) and abundant sulfate. Presence of K^+ signal was found in the OC particles suggesting possible biomass burning sources (Bi et al. 2011). The Pb particles showed its typical ions at m/z $208Pb^+$ and internally mixed with K^+ and Cl^-. Previous studies found that K and Cl internally mixed with Pb particles have a possible origination of waste incineration (Zhang et al., 2009) or iron and steel facility (Tsai et al., 2007). Internally mixed EC with metal signatures was observed in the Other particles.

Previous measurements found that dust, playa salts or sea salt particles are often enriched in larger cloud droplets (~20 μm) (Bator and Collett, 1997; Pratt et al., 2010b). Organic carbon tend to be enriched in small cloud/fog droplets, extending to 4 μm (Herckes et al., 2013). It is wealth to note that cloud droplets were above 8 μm in the present study. Thus, it partially leads to relatively larger fractions of the Dust and Na-rich cloud residues observed, and the less fractions of the OC cloud residues.

3.3 Mixing state of secondary species in cloud residues

The Nf of sulfate-containing particles were found to be highly related to the K-rich (91%), OC (100%), aged EC (98%), Pb (74%), Fe (93%) and Amine (99%) cloud residues, as shown in Figure 5. Lower Nf of sulfate-containing particles were observed in the Na-rich (41%) and Dust (42%) cloud residues. In contrast, nitrate-containing particles contributed 89% and 88% by number to the Na-rich and Dust cloud residues, respectively. The heterogeneous chemistry of HNO_3 in the Na-rich and Dust particles may lead to the preferential enrichment of nitrate (Li and Shao, 2009). Note that after activation, uptake of gas-phase HNO_3 would increase nitrate level in the cloud residues (Schneider et al., 2017). The detection of nitrate in the cloud residues was thought to be the form of ammonium-nitrate by estimating the ratio of m/z 30 to m/z 46 in AMS data (Drewnick et al., 2007; Hayden et al., 2008). Low portions of ammonium (m/z, $18NH_4^+$) in the Na-rich (23% by number) and Dust (15% by number) cloud residues suggest that in this region, ammonium nitrate was not a predominant form of nitrate in the two cloud residual type. The Na-rich and Dust types were mainly composed of alkaline ion peaks (m/z, $23Na^+$, $39K^+$ and $40Ca^+$) in the position mass spectra (Figure 3), accompanied with larger fraction (88-89%) of nitrate. It suggests that nitrate might exist in the form of $Ca(NO_3)_2$, $NaNO_3$ or KNO_3 in the Dust and Na-rich cloud residues. It should be noted that the evaporation chamber of the GCVI may lead to a reduction of ammonium nitrate in the cloud residues (Hayden et al., 2008). We found that nitrate-containing particles accounted for only 46% by number of the aged EC cloud residues, which is significantly less than the contribution of sulfate-containing particles. Previous studies found that aged EC (soot) fog/cloud residues are

mainly internally mixed with sulfate (Pratt et al., 2010a; Harris et al., 2014; Bi et al., 2016). Aged EC particles mixed with sulfate are good CCN, rather than formed by in-cloud processing (Bi et al., 2016; Roth et al., 2016). High portions (75-86% by number) of ammonium-containing particles were observed for the OC and aged EC cloud residues, suggesting that ammonium will mostly be in the form of ammonium sulfate or ammonium nitrate for the two cloud residue types (Zhang et al., 2017). This result also implies that ammonium-containing particles are preferentially activated or enhanced by uptake of gaseous NH_3 to neutralize acidic cloud droplets for the OC and EC types.

Organics (e.g., amine and oxalate) have previously been measured in cloud water/residues (Sellegri et al., 2003; Sorooshian et al., 2007a; Pratt et al., 2010a). Amine and oxalate particles with mixtures of inorganic salts could enhance water uptake behavior (Sorooshian et al., 2008; Wu et al., 2011). The presence of TMA in the Amine cloud residues is expected to promote water uptake in sub- and supersaturated regimes (Sorooshian et al., 2007b). A total of 3,410 oxalate-containing particles (m/z, -89$HC_2O_4^-$) represented 14.4% by number of the total cloud residues, which was mainly associated with the K-rich cloud residues (~70% by number). Note that after activation, gas phase partitioning into condensed phase or in-cloud production pathways would increase oxalate level in cloud droplets (Sellegri et al., 2003; Pratt et al., 2010a). Relative high portions (~30% by number) of oxalate-containing particles in the metal (Pb, Fe) cloud residues might be the form of metal oxalate complexes from reactions of in-cloud formation oxalate with metals (Furukawa and Takahashi, 2011). Oxalate can readily partition into the particle phase to form amine salts (Pratt et al., 2009), it may facilitate the entrainment of oxalate (33% by number) in the Amine residues. A low fraction (4%) of oxalate-containing

particles in the OC type is a result of restrictive classification. Classification of the OC particles mainly based on intense organic carbon ion signals (e.g., m/z 27$C_2H_3^+$, 37C_3H^+, 43$C_2H_3O^+$ and 51$C_4H_3^+$). However, majority of oxalate-containing particles internally mixed with the K-rich type. Therefore, oxalate was classified to the K-rich type, probably contributed from biomass burning. Noted that K-rich could contain a large abundant of organics (Pratt et al. 2011), however, the signals of organics were covered by the potassium due to its high sensitive to the laser.

3.4 Comparison of cloud residues in different air mass sources

Figure 6 displays hourly detected particle counts and Nf values of nine types of cloud residues and ambient particles. A very abrupt increase (decrease) in Nf of aged EC (Amine) particle types from cloud residues to ambient particles was observed on Jan 17. Ambient RH showed an abrupt decrease from nearly 100% at 10:00 to 85% at 11:00 on 17 Jan (Figure 1). Ambient temperature also decreased from 10 ℃ at 11:00 to 4 ℃ at 18:00 on 17 Jan (Figure 1). These changes imply that the air mass changed from southwesterly cloudy air to northerly cloud-free air around noon on 17 Jan (Figure 2). The entrained particles originated from northern air mass might have insufficient supersaturation to activate as cloud droplets. It is the reason that Nf of particle types abruptly varied from cloud residues to ambient particles on Jan 17 (Figure 6).

Ambient RH increased from 60% at 19:00 to nearly 100% at 21:00 on 18 Jan (Figure 1). Ambient temperature also increased from 1.3 ℃ at 22:00 on 18 Jan to 3.2 ℃ at 06:00 on 19 Jan (Figure 1). These changes imply that the air mass changed from northerly cloud-free air to southwesterly cloudy air at night on 18 Jan (Figure 2). During 18-19 Jan, the

cloud residues and ambient particles showed similar chemical characteristics and were dominated by aged EC particles (Figure 6). A lack of significant variation in the Nf of particle types for this period suggests that nuclei particles originated from northerly cloud-free air could be activated to become cloud droplets. Note that ambient particles when a cloud-free event occurred at 11:00-17:00 on 19 Jan with a remaining high level of $PM_{2.5}$ (~ 22.7 μg m^{-3}). Southwesterly wind flow on 19-20 Jan was too weak (~ 2.75 m s^{-1}) to dilute particles originated from northerly air masses (Figure 1). Additionally, high RH (90%) air mass at height 1,500 m (a.s.l.) gradually moved to north China from 19 to 20 Jan (Figure S5). These might lead to similar residual particle types observed from 19 Jan to 20 Jan, although the site encountered southwesterly cloudy air on 19-20 Jan (Figure 2).

During 16-17 and 21-22 Jan, the cloud residues consisted of a high fraction of the Amine type, which significantly differed from the observation during 18-19 Jan. Clearly, the observations during 16-17 and 21-22 Jan were influenced by a strong southwesterly flow with a low value of $PM_{2.5}$ (~ 3 μg m^{-3}).

As mentioned above, the Nf of the cloud residue types significantly changed as the air mass origin varied from northerly to southwesterly. To further investigate the influence of air mass history, we selected cloud residues that had arrived from a northerly air mass on 18-19 Jan and compared these to cloud residues originating from a southwesterly air mass during the periods of 16-17 and 21-22 Jan. The detected number of cloud residues for the northerly and southwesterly air masses are given in Table S1. Note that southwesterly air mass accompanied by high relative humidity (90%) (Figure S5) may have triggered particles activated to CCN prior to their arrival to the sampling site.

The K-rich type was found to contribute 23.9% to the cloud residues in the northerly air mass, which was significantly lower than its contribution to the southwesterly air mass (51.5%), as shown in Figure 7. A similarity in averaged mass spectrum of the K-rich residues was found for the southwesterly and northerly air masses (Figure S6). The considerable increase of K-rich cloud residues suggests a major influence of regional biomass-burning activities. Biomass-burning emissions from Southeast Asia, including Myanmar, Vietnam, Laos and Thailand, where abundant fire dots are observed (Figure 2), could have been transported to the sampling site under a southwesterly air mass (Duncan et al., 2003). In contrast, the aged EC type represented only 23.7% of the cloud residues under the influence of the southwesterly air mass, which was significantly lower than observations for the northerly air mass (59.9%), as shown in Figure 7. This result suggests that the northern air mass has a greater influence on the presence of aged EC cloud residues.

In addition, an obvious increase in Nf of the Amine type was observed in the southwesterly air mass (15.1%) compared to the northerly air mass (0.2%), as shown in Figure 7. This implies that the sources or formation mechanisms of amine in cloud residues varied in different air masses. The southwesterly air mass arrived from as far as the Bay of Bengal and then travelled through Southeast Asia before reaching South China (Figure 2). The potential gas amine emissions from ocean (Facchini et al., 2008) and livestock areas (90 million animals, data was available at the website http://faostat3.fao.org) in Southeast Asia might promote the enrichment of amine particles. Note that after activation, the partitioning of the gas amine on cloud droplets may further contribute to the enhanced Amine cloud residues (Rehbein et al., 2011), especially for air masses delivered via routes with high relative humidity, as mentioned above (Figure S5). In contrast, northerly air mass

accompanied with dry airstreams may inadequately induce the partitioning of gas amines into the particle phase (Rehbein et al., 2011).

3.5 Comparison of cloud residues with ambient and non-activated particles

A direct comparison between cloud residues and ambient particles was limited because of their differences in air mass origins. During the sampling period, the cloud events occurred once the southwesterly air masses were dominant. Therefore, a comparison between cloud residues and ambient particles cannot be addressed under the influence of southwesterly air masses. Here, we chose five hours before and after the beginning of the cloud II period in order to compare cloud residues and ambient particles with similar northerly air mass origins, as discussion in Sect. 3.4. The time and detected counts of cloud residues and ambient particles for this comparison are listed in Table S1.

From 10:00 21 Jan to 13:00 23 Jan, cloud residues and non-activated particles were alternately sampled with interval of one hour. Ambient temperature decreased from 6 ℃ at 11:00 to 0 ℃ at 23:00 on 22 Jan (Figure 1). Additionally, ambient particles level (residual and non-activated particles) showed a clearly increase from 121 cm^{-3} to 1339 cm^{-3} during this period (Figure S2). It suggests that initial mixing of northerly cloud-free air and southwesterly cloudy air around noon on 22 Jan. It is noted that non-activated particles were detected in size range above 200 nm, extending to 500 nm (Figure S7). The dry northern air mass might lower supersaturation, only larger particles could be activated. This might result in above 200 nm non-activated particles observed here (Mertes et al., 2005; Kleinman et al., 2012; Hammer et al., 2014). The detected particle counts in the cloud residues and non-activated particles are given in Table S1.

463 The contribution of K-rich particles in cloud residues slightly decreased relative to
464 ambient particles (23.9% versus 30.7%), as shown in Figure 7. Previous studies also
465 showed that no significant change in Nf of biomass-burning particles for cloud residues
466 relative to ambient particles (Pratt et al., 2010a; Roth et al., 2016). The biomass-burning
467 particles internally mixed with soluble species (e.g., sulfate, nitrate and oxalate) enhanced
468 their ability to act as CCN, as discussion in Sect. 3.3. However, Kamphus et al. (2010)
469 reported that biomass-burning particles account for only 3% of cloud residues compared
470 with 43% of ambient particles, and they suspected that biomass-burning particles might
471 exist in the form of tar balls (hydrophobic materials). A slight increase in Nf of the aged
472 EC cloud residues was observed relative to ambient particles (59.9% versus 53.8%), as
473 shown in Figure 7. In general, freshly emitted EC particles are less hydrophilic and do not
474 active as CCN (Bond et al., 2013). The aged EC particles show a high degree of internal
475 mixing with secondary inorganic compounds in this study (Figure 5), improving their
476 ability to act as CCN. The remaining particle types showed no clear differences in Nf
477 between cloud residues and ambient particles.
478 In comparing the cloud residues with non-activated particles, a significant change in Nf
479 was found for the aged EC and K-rich type. A higher Nf of K-rich particles and a lower Nf
480 of EC particles were found for the cloud residues relative to the non-activated particles
481 (Figure 7). Entrainment of northerly cloud-free air might lower supersaturation during this
482 period. Aged EC particles may require very high supersaturation to grow into cloud
483 droplets and thus, only form hydrated non-activated aerosol (Hallberg et al., 1994).
484 Figure 8 and 9 show differences in average mass spectra for cloud residues versus
485 ambient particles, as well as cloud residues versus non-activated particles, respectively.

Nitrate intensity (average ion peak area) was found to enhance in the cloud residues compared to ambient particles. In addition, nitrate-containing particles has been observed to account for 70% of the cloud residues compared to 38% of the ambient particles. Drewnick et al. (2007) suggested that rather than sulfate, high nitrate content in pre-existing particles preferentially acted as cloud droplets. Compared with containing-nitrate ambient particles, larger size of containing-nitrate residues (Figure S8) is more likely to be uptake of gaseous HNO_3 during cloud process (Hayden et al. 2008; Roth et al., 2016). A recent study also confirmed that uptake of gaseous HNO_3 was an important contributor for increasing in nitrate level in the cloud residues (Schneider et al., 2017). Interestingly, we observed a decrease in nitrate intensity in cloud residues except dust type (Figure 9) and a large size distribution of nitrate-containing cloud residues (Figure S7) compared with non-activated particles. This result suggests that particle size, rather than nitrate content, plays a more important role in the activation of particles into cloud droplets.

Sulfate intensity was only observed to enhance for the OC cloud residues relative to both ambient and non-activated particles. Although the in-cloud addition of sulfate can be produced from aqueous Fe-catalyzed or oxidation by H_2O_2/O_3 reactions (Harris et al., 2014), sulfate intensity was found to diminish in the Fe cloud residues relative to ambient particles. Compared with non-activated particles, sulfate intensity was found to enhance in the Fe cloud residues. Additionally, sulfate-containing particles accounted for 94%, 93% and 94% of cloud residues, ambient and non-activated particles, respectively. Previous studies also showed that the mass or number fraction of sulfate-containing particles in the cloud residues changed between ambient and non-activated particles (Drewnick et al., 2007; Twohy and Anderson, 2008; Schneider et al., 2017). However, the reason for these changes

remains unclear.

The in-cloud process has been reported to be an important pathway for the production of amine particles (Rehbein et al., 2011; Zhang et al., 2012a). In this study, no remarkable change in Nf of the Amine cloud residues was obtained relative to the ambient particles (0.2% versus 0.2%), as shown in Figure 7. Bi et al. (2016) considered that the absence of amine species in fog residues may be partially affected by droplet evaporation in the GCVI. We did find a high fraction of the Amine cloud residues when the southwesterly air mass prevailed, as discussion in Sect. 3.4. A lack of gas-phase amines may be the cause of few amine particles detected in the ambient particles and cloud residues (Rehbein et al., 2011). An increase in Nf of cloud residues was observed compared with non-activated particles (5.2% versus 0.1%), as shown in Figure 7. Increasing the particle water content facilitates partitioning of gas-phase amine species into the aqueous phase when gas-phase amines present (Rehbein et al., 2011).

4 Conclusions

This study presented an in situ observation of individual cloud residues, non-activated and ambient particles at a mountain site in South China. The finding shows that internal mixing with soluble species (e.g., sulfate) in EC particles was an important contributor to cloud residues in a remote area of China. Change in Nf of the cloud residue types influenced by various air masses highlights the important role of regional transportation in the observed cloud residual chemistry. Initial mixing of northerly cloud-free air and southwesterly cloudy air can induce the activation of the nuclei particles to become cloud droplets. Higher fractions of nitrate (88-89% by number) were found in the Dust and Na-rich cloud residues

relative to sulfate (41-42%) and ammonium (15-23%). Higher fraction, intensity (average ion peak area) and larger size of nitrate-containing particles were found in the cloud residues relative to the ambient particles. This result is most likely the cause of the uptake from gas-phase HNO_3.

Acknowledgments

This work was supported by the National Nature Science Foundation of China (No. 91544101 and 41405131), the National Key Research and Development Program of China (SQ2017ZY01014804) and the Foundation for Leading Talents of the Guangdong Province Government. The authors thank Ji Ou from Shaoguan city Environmental Monitoring Center for the support at the observed site. We also acknowledge the NOAA Air Resources Laboratory (ARL) for the provision of the HYSPLIT transport and dispersion model and/or READY website (http://ready.arl.noaa.gov) used in this publication. All the data can be obtained by contacting the corresponding author.

References

Andreae, M. O. and Rosenfeld, D.: Aerosol-cloud-precipitation interactions. Part 1. The nature and sources of cloud-active aerosols, Earth-Sci. Revi., 89, 13-41, doi: 10.1016/j.earscirev.2008.03.001, 2008.

Angelino, S., Suess, D.T. and Prather, K. A.: Formation of aerosol particles from reactions of secondary and tertiary alkylamines: Characterization by aerosol time-of-flight mass spectrometry, Environ. Sci. Technol., 35, 3130-3138, doi: 10.1021/es0015444, 2001.

554 Bator, A. and Collett, J.L.: Cloud chemistry varies with drop size, J. Geophys. Res. Atmos.,
555 102, 28071-28078. 1997.
556 Bi, X., Lin, Q., Peng, L., Zhang, G., Wang, X., Brechtel, F. J., Chen, D., Li, M., Peng, P.
557 a., Sheng, G. and Zhou, Z.: In situ detection of the chemistry of individual fog droplet
558 residues in the Pearl River Delta region, China, J. Geophys. Res. Atmos., 121(15), 9105-
559 9116, doi:10.1002/2016jd024886, 2016.
560 Bi, X., Zhang, G., Li, L., Wang, X., Li, M., Sheng, G., Fu, J. and Zhou, Z.: Mixing state of
561 biomass burning particles by single particle aerosol mass spectrometer in the urban area
562 of PRD, China. Atmos. Environ., 45, 3447-3453, doi:10.1016/j.atmosenv.2011.03.034,
563 2011.
564 Berg, L.K., Berkowitz, C.M., Hubbe, J.M., Ogren, J.A., Hostetler, C.A., Ferrare, R.A., Hair,
565 J.W., Dubey, M.K., Mazzoleni, C. and Andrews, E.: Overview of the cumulus humilis
566 aerosol processing study, B. Am. Meteorol. Soc. 90, 1653-1667,
567 http://dx.doi.org/10.1175/2009BAMS2760.1, 2009.
568 Bond, T. C., Doherty, S. J., Fahey, D. W., Forster, P. M., Berntsen, T., DeAngelo, B. J.,
569 Flanner, M. G., Ghan, S., Kärcher, B., Koch, D., Kinne, S., Kondo, Y., Quinn, P. K.,
570 Sarofim, M. C., Schultz, M. G., Schulz, M., Venkataraman, C., Zhang, H., Zhang, S.,
571 Bellouin, N., Guttikunda, S. K., Hopke, P. K., Jacobson, M. Z., Kaiser, J. W., Klimont,
572 Z., Lohmann, U., Schwarz, J. P., Shindell, D., Storelvmo, T., Warren, S. G. and Zender,
573 C. S.: Bounding the role of black carbon in the climate system: A scientific assessment,
574 J. Geophys. Res. Atmos., 118, 5380-5552, doi:10.1002/jgrd.50171, 2013.
575 Boucher, O., Randall, D., Artaxo, P., Bretherton, C., Feingold, G., Forster, P., Kerminen,
576 V., Kondo,Y., Liao, H., Lohmann, U., Rasch, P., Satheesh, S., Sherwood, S., Stevens, B.

577 and Zhang X.: Clouds and Aerosols. In Climate Change 2013: The Physical Science
578 Basis. Contribution of Working Group I to the Fifth Assessment Report of the
579 Intergovernmental Panel on Climate Change [Stocker, T.F., D. Qin, G.-K. Plattner, M.
580 Tignor, S.K. Allen, J. Boschung, A. Nauels, Y. Xia, V. Bex and P.M. Midgley (eds.)].
581 Cambridge University Press, Cambridge, United Kingdom and New York, NY, USA.
582 2013
583 Coggon, M.M., Sorooshian, A., Wang, Z., Craven, J.S., Metcalf, A.R., Lin, J.J., Nenes, A.,
584 Jonsson, H.H., Flagan, R.C. and Seinfeld, J.H.: Observations of continental biogenic
585 impacts on marine aerosol and clouds off the coast of California, J. Geophys. Res.
586 Atmos., 119, 6724-6748. doi:10.1002/2013JD021228, 2014.
587 Cziczo, D.J., Murphy, D.M., Hudson, P.K. and Thomson, D.S.: Single particle
588 measurements of the chemical composition of cirrus ice residue during CRYSTAL-
589 FACE, J. Geophys. Res. Atmos., 109, D04201, doi:10.1029/2003JD004032, 2004.
590 Cziczo, D.J., Froyd, K.D., Hoose, C., Jensen, E.J., Diao, M., Zondlo, M.A., Smith, J.B.,
591 Twohy, C.H. and Murphy, D.M.: Clarifying the dominant sources and mechanisms of
592 cirrus cloud formation, Science, 340, 1320-1324. doi: 10.1126/science.1234145,2013.
593 Drewnick, F., Schneider, J., Hings, S. S., Hock, N., Noone, K., Targino, A., Weimer, S.
594 and Borrmann, S.: Measurement of ambient, interstitial, and residual aerosol particles
595 on a mountaintop site in central Sweden using an aerosol mass spectrometer and a CVI,
596 J. Atmos. Chem., 56, 1-20, doi:10.1007/s10874-006-9036-8, 2007.
597 Deng, X., Wu, D., Shi, Y., Tang, H., Fan, S., Huang, H., Mao, W. and Ye, Y.:
598 Comprehensive analysis of the macro-and micro-physical characteristics of dense fog in

599 the area south of the Nanling Mountains (in Chinese), J.Trop. Meteorol., 23, 424-434.
600 2007.
601 Duncan, B. N., Martin, R. V., Staudt, A. C., Yevich, R. and Logan, J. A.: Interannual and
602 seasonal variability of biomass burning emissions constrained by satellite observations,
603 J. Geophys. Res. Atmos., 108(D2), doi:108, 10.1029/2002jd002378, 2003.
604 Freud, E., Rosenfeld, D., Andreae, M.O., Costa, A.A. and Artaxo, P.: Robust relations
605 between CCN and the vertical evolution of cloud drop size distribution in deep
606 convective clouds, Atmos. Chem. Phys., 8, 1661-1675, 2008.
607 Facchini, M. C., Decesari, S., Rinaldi, M., Carbone, C., Finessi, E., Mircea, M., Fuzzi, S.,
608 Moretti, F., Tagliavini, E. and Ceburnis, D.: Important source of marine secondary
609 organic aerosol from biogenic amines, Environ. Sci. Technol., 42, 9116-9121, doi:
610 10.1021/es8018385, 2008.
611 Furukawa, T. and Takahashi, Y.: Oxalate metal complexes in aerosol particles:
612 implications for the hygroscopicity of oxalate-containing particles, Atmos. Chem. Phys.,
613 11, 4289-4301, doi:10.5194/acp-11-4289-2011, 2011.
614 Hallberg, A., Ogren, J. A., Noone, K. J., Okada, K., Heintzenberg, J. and Svenningsson, I.
615 B.: The influence of aerosol particle composition on cloud droplet formation, J. Atmos.
616 Chem., 19, 153-171, doi: 10.1007/978-94-011-0313-8_8,1994.
617 Harris, E., Sinha, B., van Pinxteren, D., Tilgner, A., Fomba, K. W., Schneider, J., Roth, A.,
618 Gnauk, T., Fahlbusch, B. and Mertes, S.: Enhanced role of transition metal ion catalysis
619 during in-cloud oxidation of SO_2, Science, 340, 727-730, doi:10.1126/science.1230911,
620 2013.

621 Harris, E., Sinha, B., van Pinxteren, D., Schneider, J., Poulain, L., Collett, J., D'Anna, B.,
622 Fahlbusch, B., Foley, S., Fomba, K. W., George, C., Gnauk, T., Henning, S., Lee, T.,
623 Mertes, S., Roth, A., Stratmann, F., Borrmann, S., Hoppe, P. and Herrmann, H.: In-cloud
624 sulfate addition to single particles resolved with sulfur isotope analysis during HCCT-
625 2010, Atmos. Chem. Phys., 14, 4219-4235, doi:10.5194/acp-14-4219-2014, 2014.
626 Hammer, E., Gysel, M., Roberts, G.C., Elias, T., Hofer, J., Hoyle, C.R., Bukowiecki, N.,
627 Dupont, J.C., Burnet, F., Baltensperger, U. and Weingartner, E.: Size-dependent particle
628 activation properties in fog during the ParisFog 2012/13 field campaign, Atmos. Chem.
629 Phys., 14, 10517-10533, 2014.
630 Hayden, K. L., Macdonald, A. M., Gong, W., Toom-Sauntry, D., Anlauf, K. G., Leithead,
631 A., Li, S. M., Leaitch, W. R. and Noone, K.: Cloud processing of nitrate, J. Geophys.
632 Res. Atmos., 113(D18), doi:10.1029/2007jd009732, 2008.
633 Herich, H., Kammermann, L., Gysel, M., Weingartner, E., Baltensperger, U., Lohmann, U.
634 and Cziczo, D. J.: In situ determination of atmospheric aerosol composition as a function
635 of hygroscopic growth, J. Geophys. Res. Atmos., 113(D16), doi:10.1029/2008jd009954,
636 2008.
637 Herckes, P., Valsaraj, K.T. and Collett, J.L., A review of observations of organic matter in
638 fogs and clouds: Origin, processing and fate, Atmos. Res., 132, 434-449. 2013.
639 Hudson, P.K., Murphy, D.M., Cziczo, D.J., Thomson, D.S., de Gouw, J.A., Warneke, C.,
640 Holloway, J., Jost, H.J. and Hübler, G.: Biomass-burning particle measurements:
641 Characteristic composition and chemical processing, J. Geophys. Res. Atmos., 109,
642 D23S27, doi:10.1029/2003JD004398, 2004.

643 Kamphus, M., Ettner-Mahl, M., Klimach, T., Drewnick, F., Keller, L., Cziczo, D. J.,
644 Mertes, S., Borrmann, S. and Curtius, J.: Chemical composition of ambient aerosol, ice
645 residues and cloud droplet residues in mixed-phase clouds: single particle analysis
646 during the Cloud and Aerosol Characterization Experiment (CLACE 6), Atmos. Chem.
647 Phys., 10, 8077-8095, doi:10.5194/acp-10-8077-2010, 2010.
648 Kleinman, L.I., Daum, P.H., Lee, Y.-N., Lewis, E.R., Sedlacek III, A., Senum, G.,
649 Springston, S., Wang, J., Hubbe, J. and Jayne, J.: Aerosol concentration and size
650 distribution measured below, in, and above cloud from the DOE G-1 during VOCALS-
651 Rex, Atmos. Chem. Phys., 12, 207-223, 2012.
652 Lee, C. S. L., Li, X., Zhang, G., Peng, X. and Zhang, L.: Biomonitoring of trace metals in
653 the atmosphere using moss (Hypnum plumaeforme) in the Nanling Mountains and the
654 Pearl River Delta, Southern China. Atmos. Environ., 39(3), 397-407, 2005.
655 Li, L., Huang, Z., Dong, J., Li, M., Gao, W., Nian, H., Fu, Z., Zhang, G., Bi, X. and Cheng,
656 P.: Real time bipolar time-of-flight mass spectrometer for analyzing single aerosol
657 particles, Int. J. Mass Spectrom., 303, 118-124,
658 doi:http://dx.doi.org/10.1016/j.ijms.2011.01.017, 2011a.
659 Li, T., Wang, Y., Zhou, J., Wang, T., Ding, A., Nie, W., Xue, L., Wang, X. and Wang, W.:
660 Evolution of trace elements in the planetary boundary layer in southern China: effects of
661 dust storms and aerosol-cloud interaction, J. Geophys. Res. Atmos., 122, 3492-3506,
662 2017.
663 Li, W., Li, P., Sun, G., Zhou, S., Yuan, Q. and Wang, W.: Cloud residues and interstitial
664 aerosols from non-precipitating clouds over an industrial and urban area in northern
665 China, Atmos. Environ., 45, 2488-2495, doi:10.1016/j.atmosenv.2011.02.044, 2011b.

666 Lohmann, U., Stier, P., Hoose, C., Ferrachat, S., Kloster, S., Roeckner, E. and Zhang, J.:
667 Cloud microphysics and aerosol indirect effects in the global climate model ECHAM5-
668 HAM, Atmos. Chem. Phys., 7, 3425-3446, 2007.
669 Matsuki, A., Schwarzenboeck, A., Venzac, H., Laj, P., Crumeyrolle, S. and Gomes, L.:
670 Cloud processing of mineral dust: direct comparison of cloud residual and clear sky
671 particles during AMMA aircraft campaign in summer 2006, Atmos. Chem. Phys., 10,
672 1057-1069, 2010.
673 McFiggans, G., Artaxo, P., Baltensperger, U., Coe, H., Facchini, M. C., Feingold, G., Fuzzi,
674 S., Gysel, M., Laaksonen, A. and Lohmann, U.: The effect of physical and chemical
675 aerosol properties on warm cloud droplet activation, Atmos. Chem. Phys., 6, 2593-2649,
676 doi:10.5194/acp-6-2593-2006, 2006.
677 Mertes, S., Lehmann, K., Nowak, A., Massling, A. and Wiedensohler, A.: Link between
678 aerosol hygroscopic growth and dropletactivation observed for hill-capped clouds at
679 connected flow conditions during FEBUKO, Atmos. Environ., 39, 4247-4256, 2005.
680 Moffet, R.C., Foy, B. D., Molina, L. A., Molina, M. and Prather, K.A.: Measurement of
681 ambient aerosols in northern Mexico City by single particle mass spectrometry, Atmos.
682 Chem. Phys., 8, 4499-4516, doi:10.5194/acp-8-4499-2008, 2008.
683 Moffet, R.C. and Prather, K.A.: In-situ measurements of the mixing state and optical
684 properties of soot with implications for radiative forcing estimates, Proc. Natl. Acad. Sci.
685 USA, 106, 11872-11877, doi: 10.1073/pnas.0900040106, 2009.
686 Pratt, K.A., Hatch, L. E. and Prather, K. A.: Seasonal volatility dependence of ambient
687 particle phase amines, Environ. Sci. Technol., 43, 5276-5281, doi:10.1021/es803189n,
688 2009.

689 Pratt, K.A., Heymsfield, A. J., Twohy, C. H., Murphy, S. M., DeMott, P. J., Hudson, J. G.,
690 Subramanian, R., Wang, Z., Seinfeld, J. H. and Prather, K. A.: In Situ Chemical
691 Characterization of Aged Biomass-Burning Aerosols Impacting Cold Wave Clouds, J.
692 Atmos. Sci., 67, 2451-2468, doi:10.1175/2010jas3330.1, 2010a.
693 Pratt, K.A., Murphy, S., Subramanian, R., DeMott, P., Kok, G., Campos, T., Rogers, D.,
694 Prenni, A., Heymsfield, A. and Seinfeld, J.: Flight-based chemical characterization of
695 biomass burning aerosols within two prescribed burn smoke plumes, Atmos. Chem.
696 Phys., 11, 12549-12565, doi:10.5194/acp-11-12549-2011, 2011.
697 Pratt, K.A., Twohy, C.H., Murphy, S.M., Moffet, R.C., Heymsfield, A.J., Gaston, C.J.,
698 DeMott, P.J., Field, P.R., Henn, T.R., Rogers, D.C., Gilles, M.K., Seinfeld, J.H. and
699 Prather, K.A.: Observation of playa salts as nuclei in orographic wave clouds, J. Geophys.
700 Res. Atmos., 115, D15301, doi:10.1029/2009JD013606, 2010b.
701 Qin, X., Bhave, P.V. and Prather, K. A.: Comparison of two methods for obtaining
702 quantitative mass concentrations from aerosol time-of-flight mass spectrometry
703 measurements, Anal. Chem., 78(17), 6169-6178, doi: 10.1021/ac060395q, 2006.
704 Rehbein, P. J., Jeong, C. H., McGuire, M. L., Yao, X., Corbin, J. C. and Evans, G. J.: Cloud
705 and fog processing enhanced gas-to-particle partitioning of trimethylamine, Environ. Sci.
706 Technol., 45, 4346-4352, doi:10.1021/es1042113, 2011.
707 Rosenfeld, D., Lohmann, U., Raga, G.B., O'Dowd, C.D., Kulmala, M., Fuzzi, S., Reissell,
708 A. and Andreae, M.O.: Flood or drought: how do aerosols affect precipitation?, Science,
709 321, 1309-1313, doi: 10.1126/science.1160606, 2008.
710 Roth, A., Schneider, J., Klimach, T., Mertes, S., van Pinxteren, D., Herrmann, H. and
711 Borrmann, S.: Aerosol properties, source identification, and cloud processing in

712 orographic clouds measured by single particle mass spectrometry on a central European
713 mountain site during HCCT-2010, Atmos. Chem. Phys., 16, 505-524, doi:10.5194/acp-
714 16-505-2016, 2016.
715 Schneider, J., Mertes, S., van Pinxteren, D., Herrmann, H. and Borrmann, S.: Uptake of
716 nitric acid, ammonia, and organics in orographic clouds: Mass spectrometric analyses of
717 droplet residual and interstitial aerosol particles, Atmos. Chem. Phys., 17, 1571-1593,
718 doi:10.5194/acp-17-1571-2017, 2017.
719 Seinfeld, J.H., Bretherton, C., Carslaw, K.S., Coe, H., DeMott, P.J., Dunlea, E.J., Feingold,
720 G., Ghan, S., Guenther, A.B. and Kahn, R.: Improving our fundamental understanding
721 of the role of aerosol-cloud interactions in the climate system, Proc. Natl. Acad. Sci.
722 USA, 113, 5781-5790, doi: 10.1073/pnas.1514043113, 2016.
723 Sellegri, K., Laj, P., Marinoni, A., Dupuy, R., Legrand, M. and Preunkert, S.: Contribution
724 of gaseous and particulate species to droplet solute composition at the Puy de Dôme,
725 France, Atmos. Chem. Phys., 3, 1509-1522, doi:10.5194/acp-3-1509-2003, 2003.
726 Shingler, T., Dey, S., Sorooshian, A., Brechtel, F. J., Wang, Z., Metcalf, A., Coggon, M.,
727 Mülmenstädt, J., Russell, L. M., Jonsson, H. H. and Seinfeld, J. H.: Characterisation and
728 airborne deployment of a new counterflow virtual impactor inlet, Atmos. Meas. Tech.,
729 5, 1259-1269, doi:10.5194/amt-5-1259-2012, 2012.
730 Song, X.H., Hopke, P. K., Fergenson, D. P. and Prather, K. A.: Classification of single
731 particles analyzed by ATOFMS using an artificial neural network, ART-2A, Anal.
732 Chem., 71, 860-865, doi:10.1021/ac9809682, 1999.
733 Sorooshian, A., Ng, N. L., Chan, A. W. H., Feingold, G., Flagan, R. C. and Seinfeld, J. H.:
734 Particulate organic acids and overall water-soluble aerosol composition measurements

735 from the 2006 Gulf of Mexico Atmospheric Composition and Climate Study
736 (GoMACCS), J. Geophys. Res. Atmos., 112(D13), doi:10.1029/2007JD008537, 2007a.
737 Sorooshian, A., Lu, M. L., Brechtel, F. J., Jonsson, H., Feingold, G., Flagan, R. C. and
738 Seinfeld, J. H.: On the source of organic acid aerosol layers above clouds, Environ. Sci.
739 Technol., 41, 4647-4654, doi: 10.1021/es0630442, 2007b.
740 Sorooshian, A., Murphy, S., Hersey, S., Gates, H., Padro, L., Nenes, A., Brechtel, F.,
741 Jonsson, H., Flagan, R. and Seinfeld, J.: Comprehensive airborne characterization of
742 aerosol from a major bovine source, Atmos. Chem. Phys., 8, 5489-5520, doi:
743 http://dx.doi.org/10.5194/acp-8-5489-2008, 2008.
744 Stier, P., Feichter, J., Kinne, S., Kloster, S., Vignati, E., Wilson, J., Ganzeveld, L., Tegen,
745 I., Werner, M. and Balkanski, Y.: The aerosol-climate model ECHAM5-HAM, Atmos.
746 Chem. Phys., 5, 1125-1156. 2005.
747 Tang, M., Cziczo, D. J. and Grassian, V. H.: Interactions of Water with Mineral Dust
748 Aerosol: Water Adsorption, Hygroscopicity, Cloud Condensation, and Ice Nucleation,
749 Chem. Rev., doi:10.1021/acs.chemrev.5b00529, 2016.
750 Targino, A.C., Krejci, R., Noone, K.J. and Glantz, P.: Single particle analysis of ice crystal
751 residuals observed in orographic wave clouds over Scandinavia during INTACC
752 experiment, Atmos. Chem. Phys., 6, 1977-1990, 2006.
753 Tsai, J.H., Lin, K.H., Chen, C.Y., Ding, J.Y., Choa, C.G. and Chiang, H.L.: Chemical
754 constituents in particulate emissions from an integrated iron and steel facility, J. Hazard.
755 Mater., 147, 111-119. 2007.
756 Twohy, C.H., Kreidenweis, S.M., Eidhammer, T., Browell, E.V., Heymsfield, A.J.,
757 Bansemer, A.R., Anderson, B.E., Chen, G., Ismail, S., DeMott, P.J. and Van Den Heever,

S.C.: Saharan dust particles nucleate droplets in eastern Atlantic clouds, Geophys. Res. Lett., 36, doi: 10.1029/2008GL035846, 2009.

Twohy, C.H. and Poellot, M.: Chemical characteristics of ice residual nuclei in anvil cirrus clouds: evidence for homogeneous and heterogeneous ice formation, Atmos. Chem. Phys., 5, 2289-2297, 2005.

Twohy C.H. and Anderson J. R.: Droplet nuclei in non-precipitating clouds: composition and size matter. Environ. Res. Lett., 3, 045002, doi:10.1088/1748-9326/3/4/045002, 2008.

Wang, H., An, J., Shen, L., Zhu, B., Xia, L., Duan, Q. and Zou, J.: Mixing state of ambient aerosols in Nanjing city by single particle mass spectrometry, Atmos. Environ., 132, 123-132, 2016.

Wang, Y., Guo, J., Wang, T., Ding, A., Gao, J., Zhou, Y., Collett, J. L. and Wang, W.: Influence of regional pollution and sandstorms on the chemical composition of cloud/fog at the summit of Mt. Taishan in northern China, Atmos. Res., 99, 434-442, doi:10.1016/j.atmosres.2010.11.010, 2011.

Wu, Z., Nowak, A., Poulain, L., Herrmann, H., and Wiedensohler, A.: Hygroscopic behavior of atmospherically relevant water-soluble carboxylic salts and their influence on the water uptake of ammonium sulfate, Atmos. Chem. Phys., 11, 12617-12626, doi:10.5194/acp-11-12617-2011, 2011.

Zelenyuk, A., Imre, D., Earle, M., Easter, R., Korolev, A., Leaitch, R., Liu, P., Macdonald, A. M., Ovchinnikov, M. and Strapp, W.: In Situ Characterization of Cloud Condensation Nuclei, Interstitial, and Background Particles Using the Single Particle Mass Spectrometer, SPLAT II†, Anal. Chem., 82, 7943-7951, doi:10.1021/ac1013892, 2010.

781 Zhang, Khalizov, A. F., Pagels, J., Zhang, D., Xue, H. and McMurry, P. H.: Variability in
782 morphology, hygroscopicity, and optical properties of soot aerosols during atmospheric
783 processing, Proc. Natl. Acad. Sci. USA, 105, 10291-10296,
784 doi:10.1073/pnas.0804860105, 2008.
785 Zhang, G., Bi, X., Chan, L. Y., Li, L., Wang, X., Feng, J., Sheng, G., Fu, J., Li, M. and
786 Zhou, Z.: Enhanced trimethylamine-containing particles during fog events detected by
787 single particle aerosol mass spectrometry in urban Guangzhou, China, Atmos. Environ.,
788 55, 121-126, doi:10.1016/j.atmosenv.2012.03.038, 2012a.
789 Zhang, G., Bi, X., Li, L., Chan, L. Y., Li, M., Wang, X., Sheng, G., Fu, J. and Zhou, Z.:
790 Mixing state of individual submicron carbon-containing particles during spring and fall
791 seasons in urban Guangzhou, China: a case study, Atmos. Chem. Phys., 13, 4723-4735,
792 doi:10.5194/acp-13-4723-2013, 2013.
793 Zhang, G., Bi, X., Lou, S., Li, L., Wang, H., Wang, X., Zhou, Z., Sheng, G., Fu, J. and
794 Chen, C.: Source and mixing state of iron-containing particles in Shanghai by individual
795 particle analysis, Chemosphere, 95, 9-16, 2014.
796 Zhang, G., Lin, Q., Peng, L., Bi, X., Lei, M., Chen, D., Brechtel, F.J., Chen, X., Yan,
797 W.,Wang, X., Peng, P., Sheng., G. and Zhou, Z.: Single particle mixing state and cloud
798 scavenging of black carbon at a high-altitude mountain site in south China, J. Geophys.
799 Res. Atmos. in revise, 2017.
800 Zhang, X., Wang, Y., Niu, T., Zhang, X., Gong, S., Zhang, Y. and Sun, J.: Atmospheric
801 aerosol compositions in China: spatial/temporal variability, chemical signature, regional
802 haze distribution and comparisons with global aerosols, Atmos. Chem. Phys., 12, 779-
803 799, doi:10.5194/acp-12-779-2012, 2012b.

804 Zhang, Y.P., Wang, X.F., Chen, H., Yang, X., Chen, J.M. and Allen, J.O.: Source
805 apportionment of lead-containing aerosol particles in Shanghai using single particle
806 mass spectrometry, Chemosphere, 74, 501-507, 2009.

807

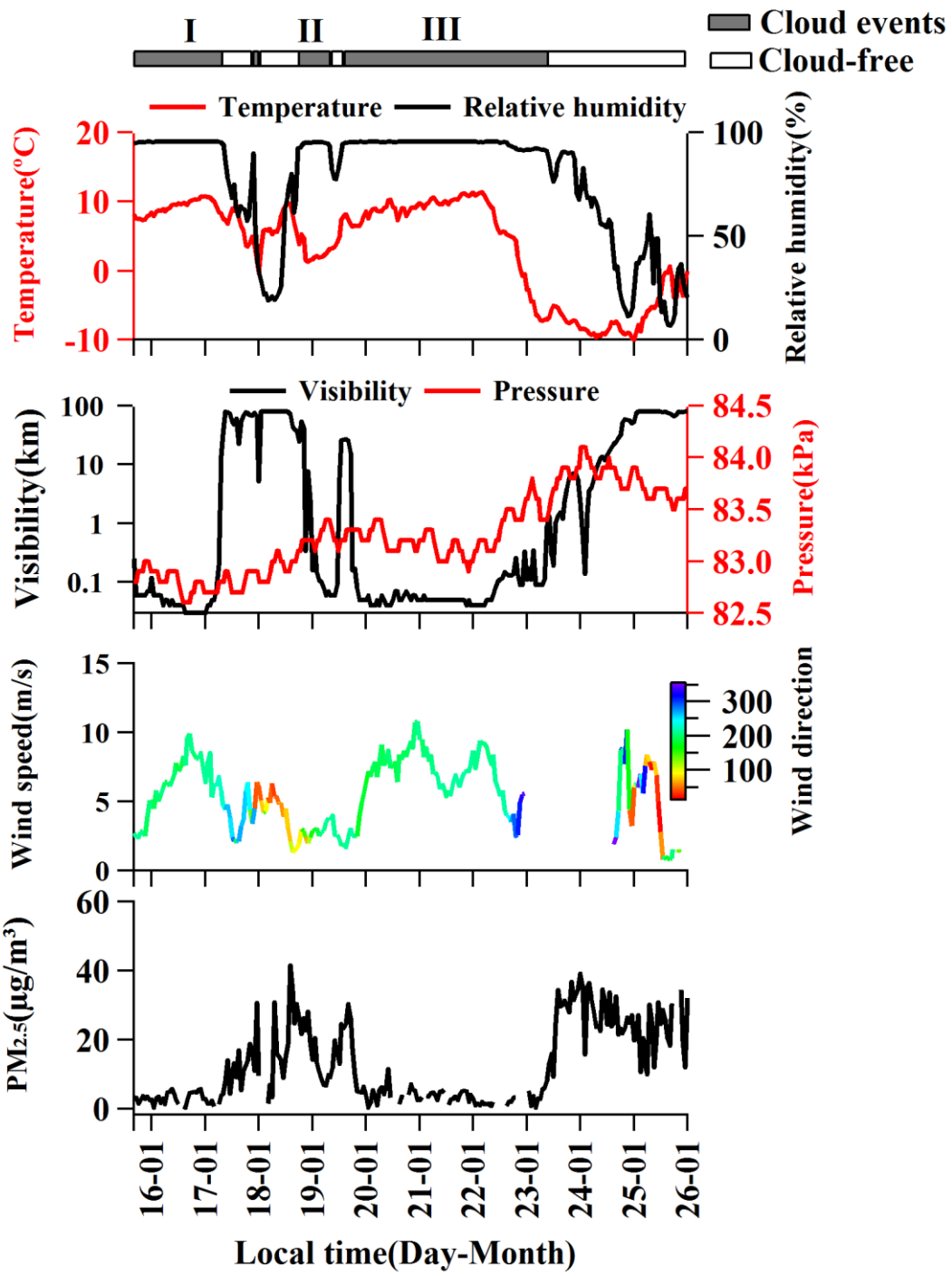

809

810 Figure 1: The hourly average variations in meteorological conditions (temperature,

811 relative humidity, visibility, pressure, wind speed and direction) and $PM_{2.5}$.

812

(a)

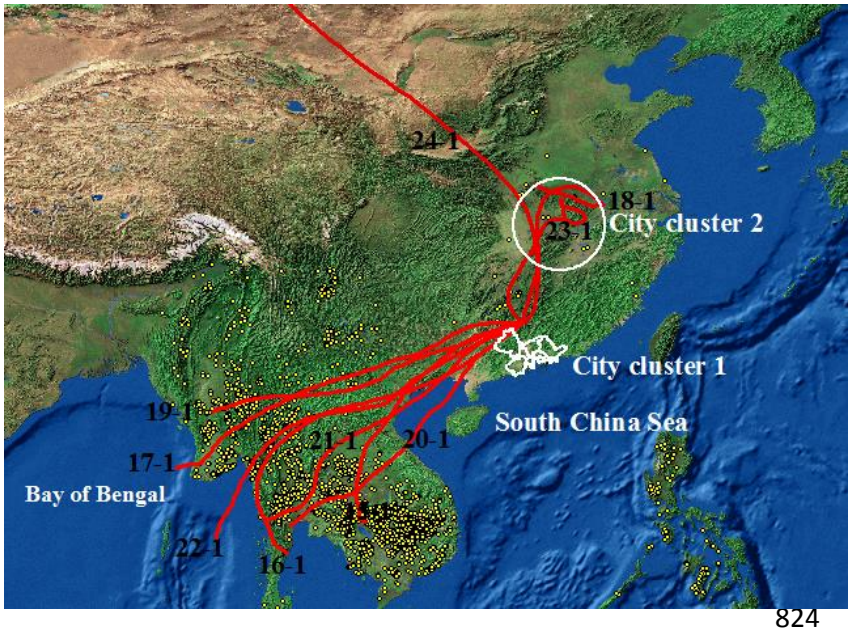

(b)

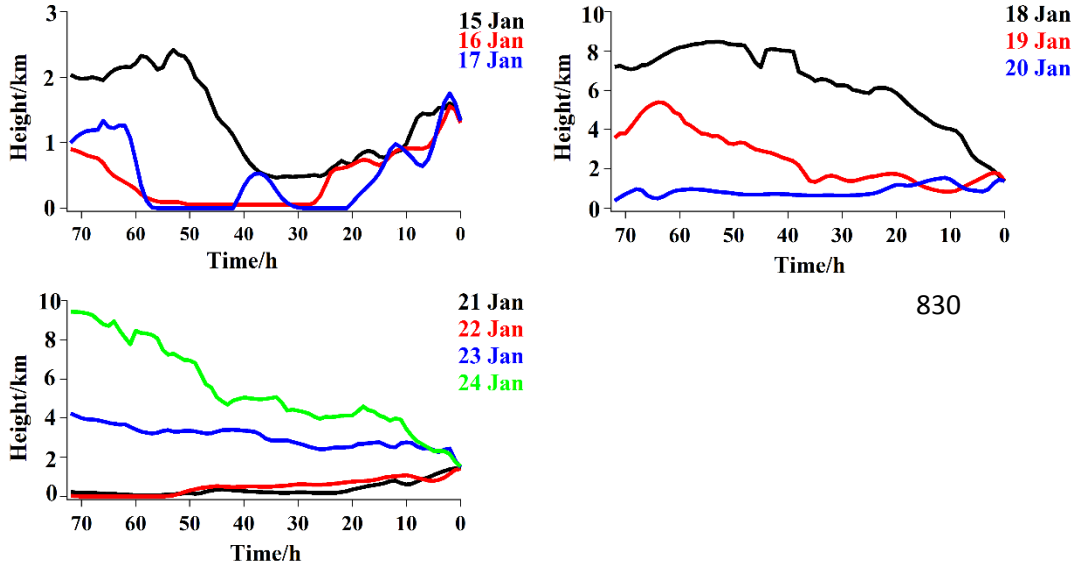

Figure 2: (a) HYSPLIT back trajectories (72 h) for air masses at 1,800 m during the whole sampling period. The white borders and circle refer to the Pearl River Delta (city cluster 1) and Yangtze River Mid-Reaches city clusters (city cluster 2), respectively. The yellow rots represent fire dots during the study periods. The fire dots are available at

838 https://earthdata.nasa.gov/; (b) Heights (above model ground) of the air masses as a
839 function of time.

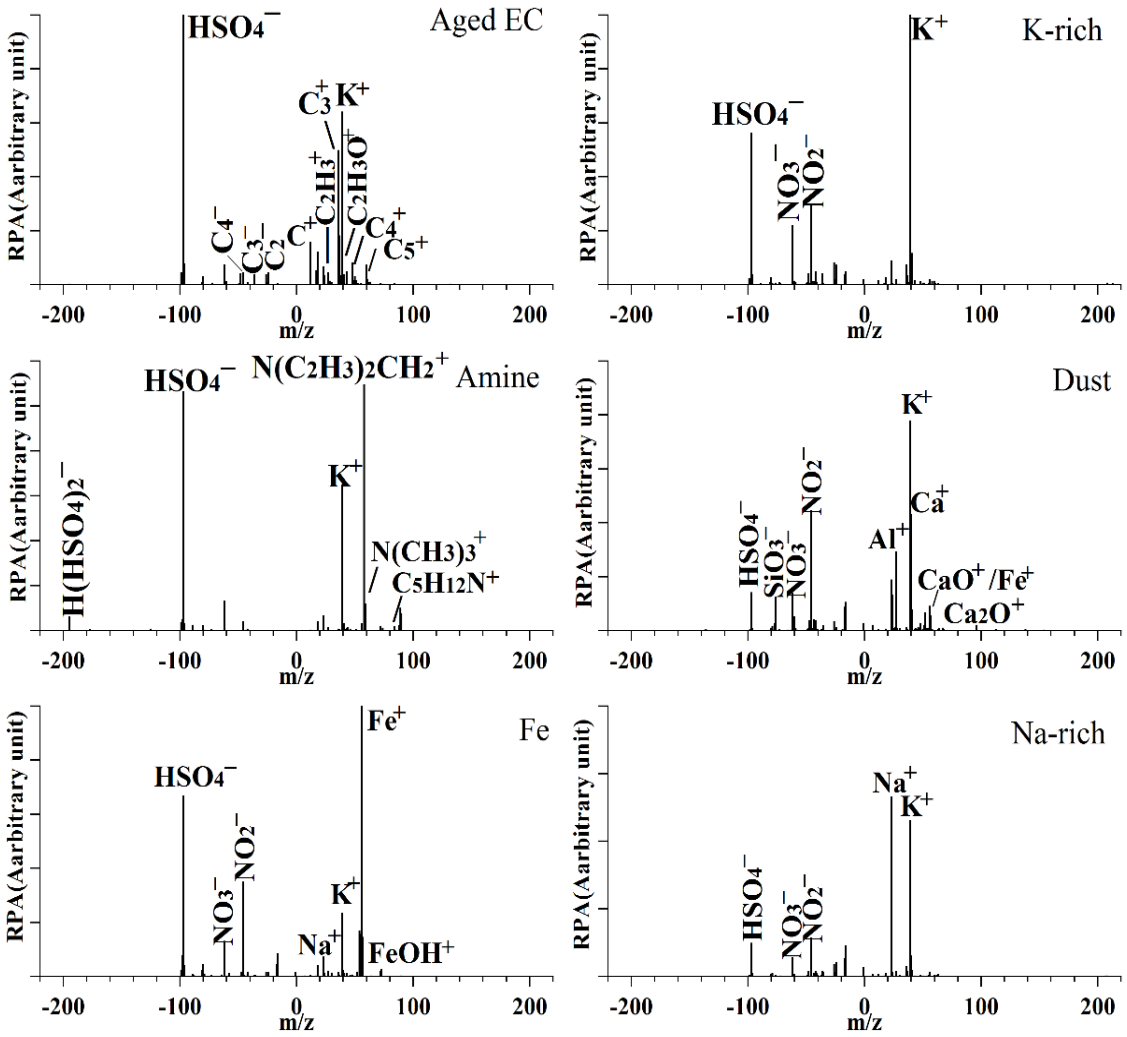

840

841 Figure 3: Averaged positive and negative mass spectra for the main 6 particle types (Aged

842 EC, K-rich, Amine, Dust, Fe, Na-rich) of the sampled particles during the whole sampling

843 period. RPA in the vertical axis refers to relative peak area. m/z in the horizontal axis

844 represents mass-to-charge ratio.

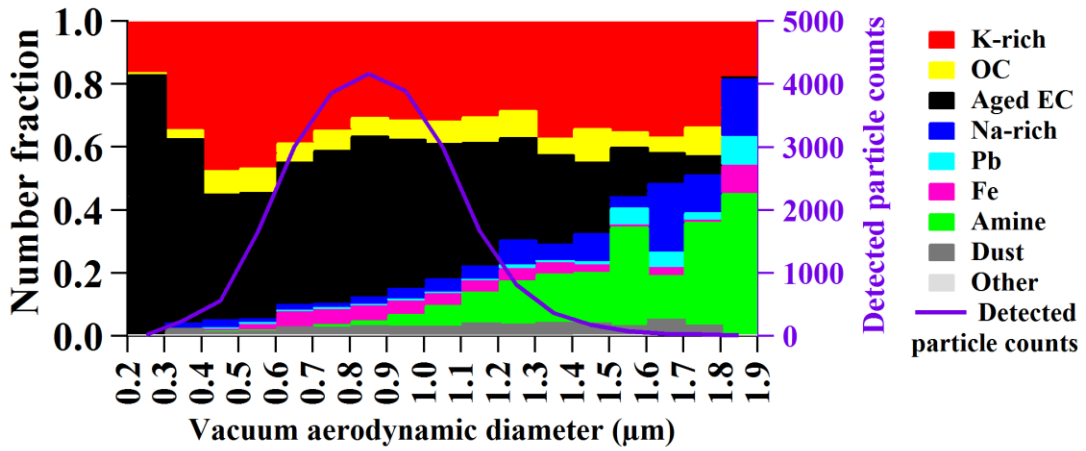

845

846 Figure 4: Number fraction for size distribution of the cloud residual types in 100 nm size

847 intervals.

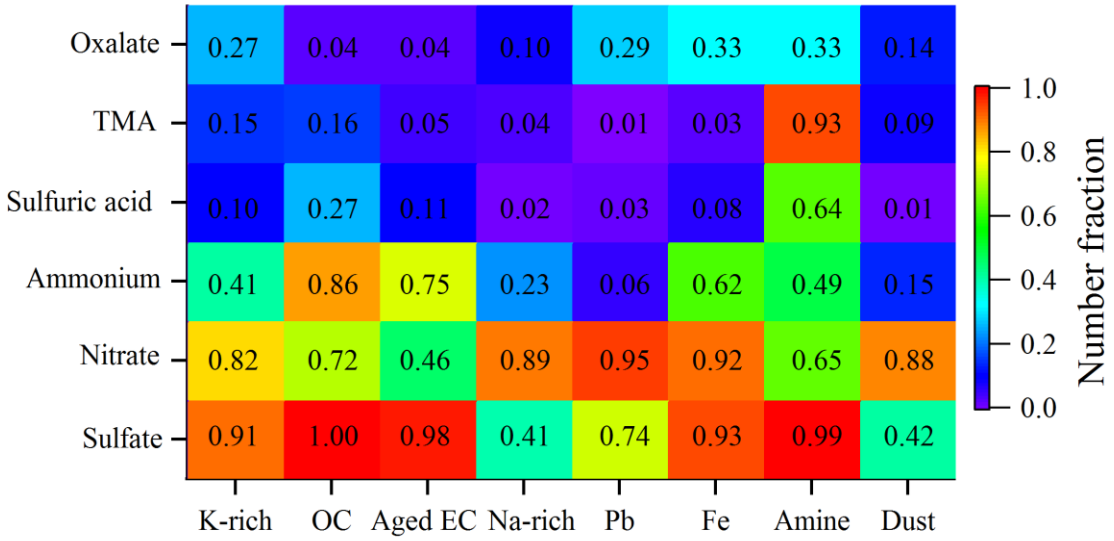

848

849 Figure 5: Mixing state of secondary markers with the total cloud residues types; Sulfate

850 (m/z, -97HSO_4^-), Nitrate (m/z, -46NO_2^- or -62NO_3^-), Ammonium (m/z, 18NH_4^+), Sulfuric

851 acid (m/z, -195$H(HSO_4)_2^-$), TMA (m/z, 59$N(CH_3)_3^+$), Oxalate (m/z, -89$HC_2O_4^-$).

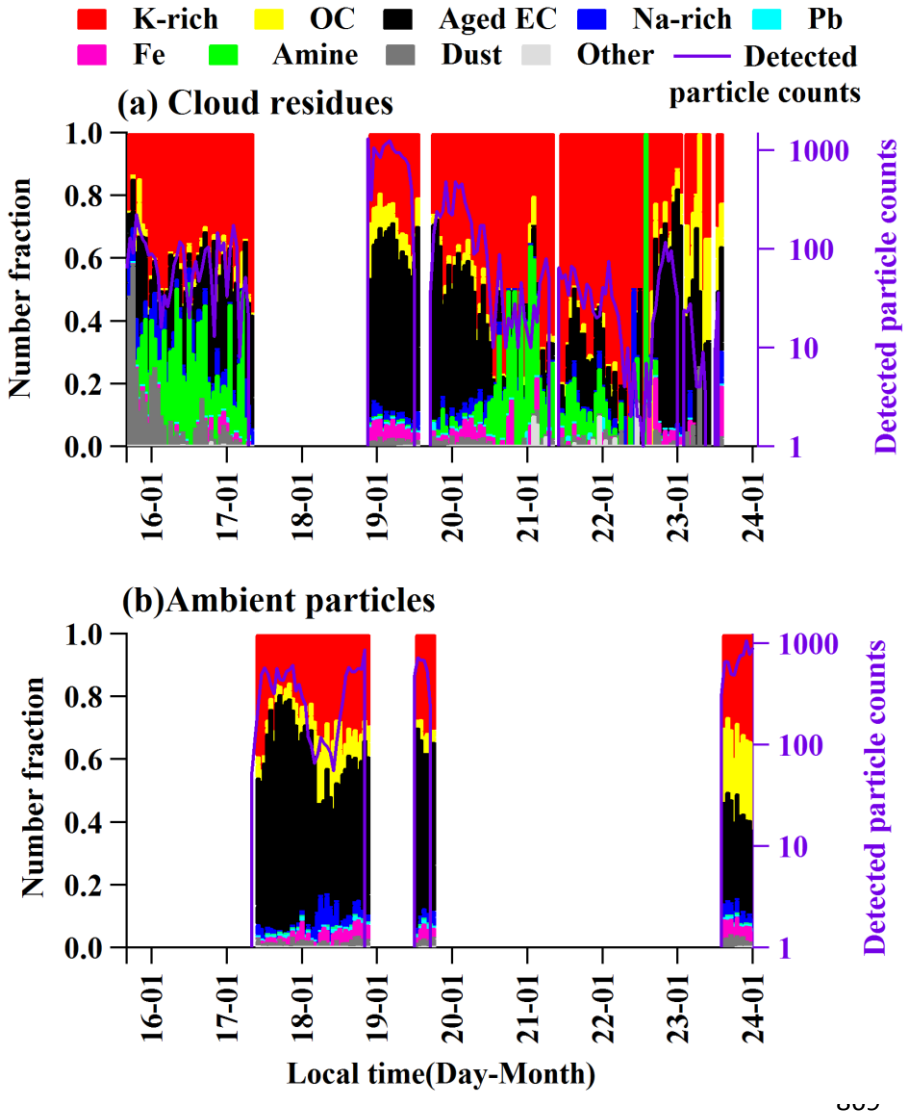

Figure 6: The hourly average variations in the cloud residual and ambient particles during the whole sampling period.

872

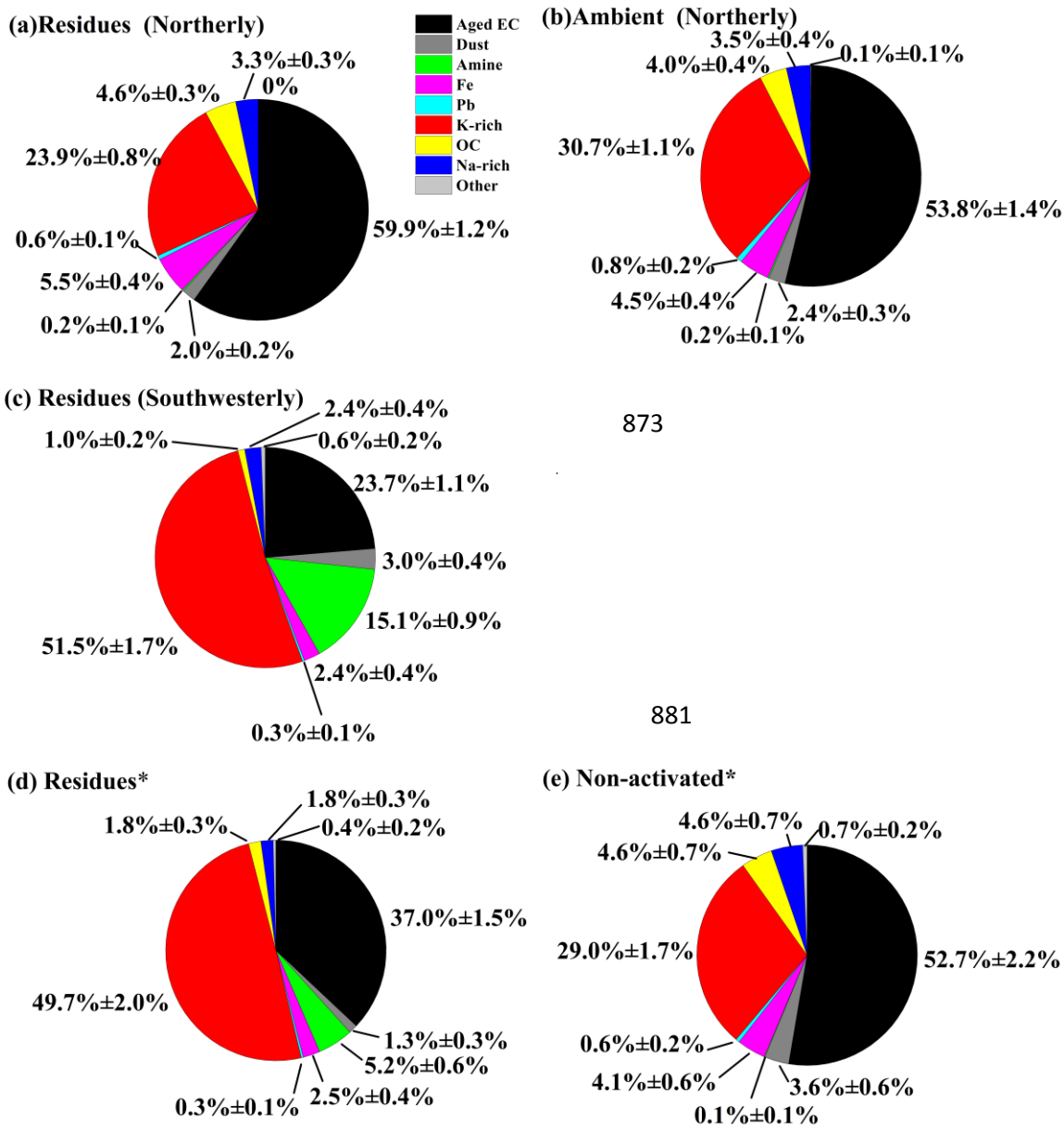

873

881

882 Figure 7: Number fraction of the cloud residues, ambient and non-activated particles. (a)
883 cloud residues during northerly air mass; (b) ambient particle during northerly air mass; (c)
884 cloud residues during southwesterly air mass; (d) cloud residues and (e) non-activated
885 particles were alternately sampled with interval of one hour during the cloud III event;
886 Uncertainties were calculated assuming Poisson statistics for analyzed particles.

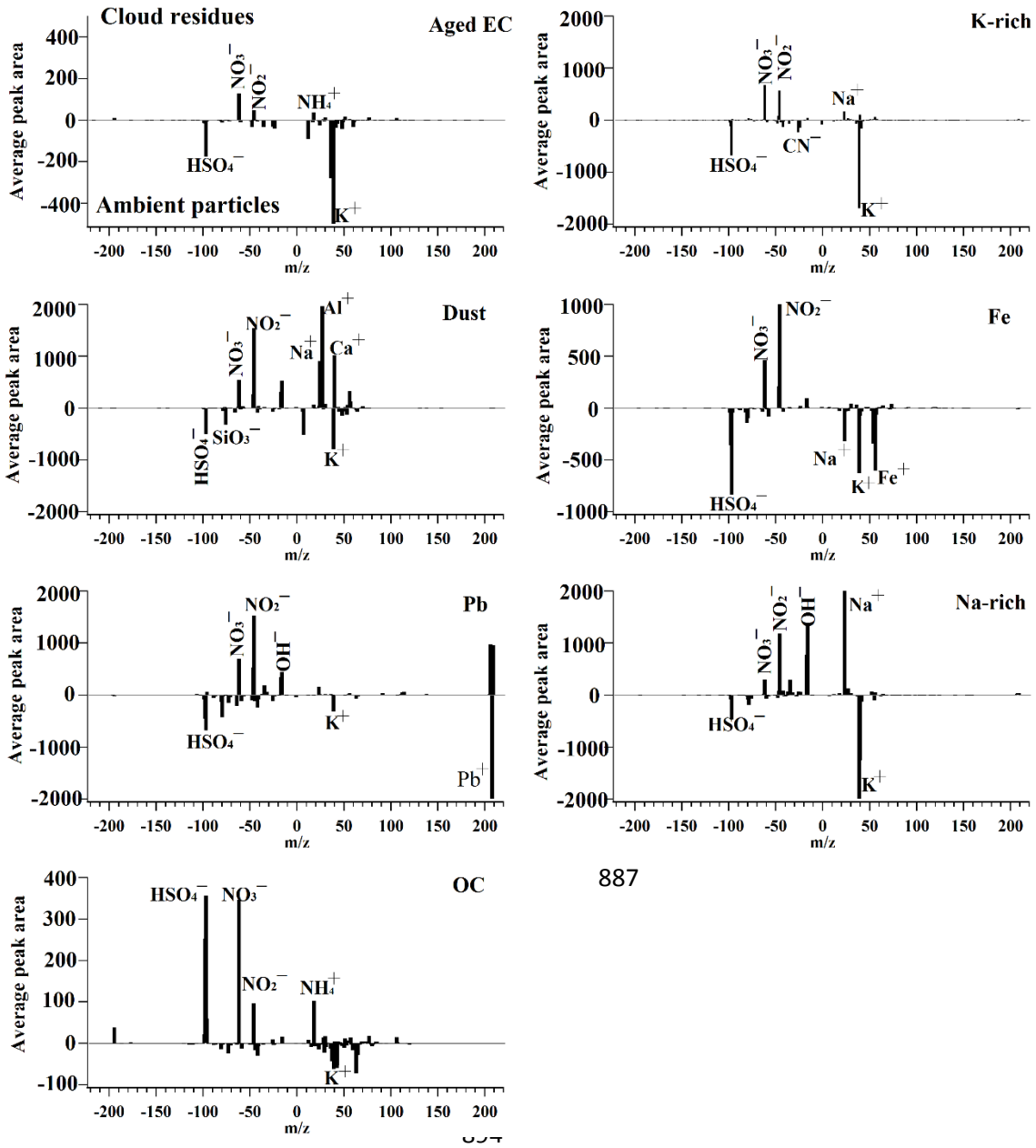

Figure 8: Mass spectral subtraction plot of the average mass spectrum corresponding to cloud residues minus ambient particles. Positive area peaks correspond to higher abundance in cloud residues, whereas negative area peaks show higher intensity in ambient particles.

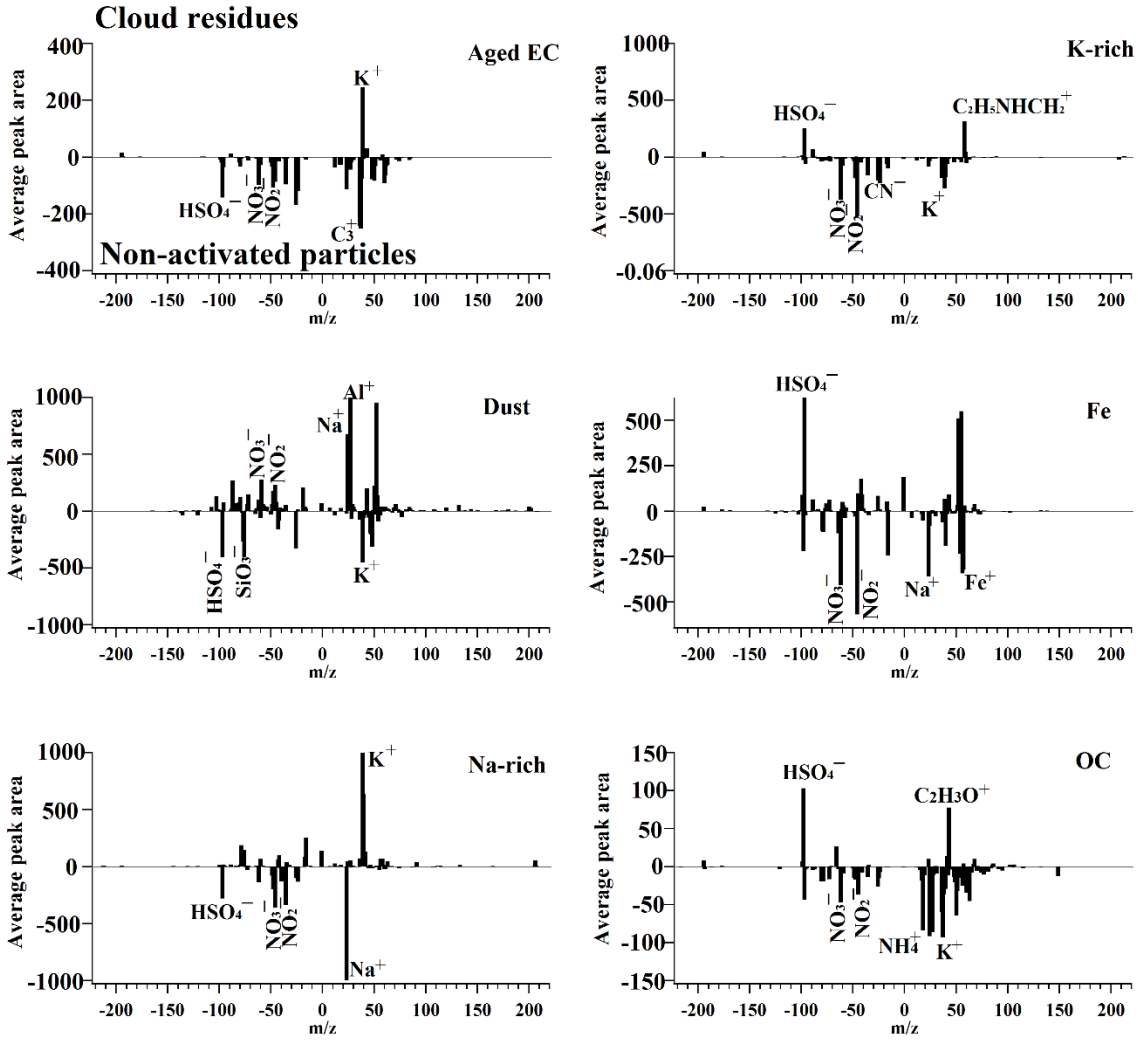

Figure 9: Mass spectral subtraction plot of the average mass spectrum corresponding to cloud residues minus non-activated particles. Positive area peaks correspond to higher abundance in cloud residues, whereas negative area peaks show higher intensity in non-activated particles.